

A Structural Basis for Restricted Codon Recognition Mediated by 2-thiocytidine in tRNA Containing a Wobble Position Inosine

Sweta Vangaveti $^{2,\dagger,\#}$, William A. Cantara $^{1,\dagger,\$}$, Jessica L. Spears 1,¶ , Hasan DeMirci 3,4 , Frank V. Murphy IV 5 , Sri V. Ranganathan 2 , Kathryn L. Sarachan $^{1,2,\parallel}$ and Paul F. Agris 1,2,‡

- 1 Department of Biological Sciences, University at Albany-SUNY, 1400 Washington Ave., Albany, NY, 12222, USA
- 2 The RNA Institute, University at Albany-SUNY, 1400 Washington Ave., Albany, NY, 12222, USA
- 3 PULSE Institute, Stanford University, 2575 Sand Hill Road, MS 59, Menlo Park, CA, 94025, USA
- 4 Department of Molecular Biology and Genetics, Koc University, Rumelifeneri yolu, Sariyer, Istanbul, 34450, Turkey
- 5 Argonne National Laboratories, NE-CAT/Cornell University, 9700 S. Cass Avenue, Lemont, IL, 60439, USA

Correspondence to Paul F. Agris, and Kathryn L. Sarachan: Paul F. Agris is to be contacted at: 203 Research Drive, DUMC 2647, Durham, NC, 27710, USA; Kathryn L. Sarachan is to be contacted at: Wilson College, 1015 Philadelphia Ave, Chambersburg, PA, 17201, USA. paul.agris@duke.edu, kathryn.sarachan@wilson.edu. https://doi.org/10.1016/j.jmb.2019.12.016

Edited by Ruben L. Gonzalez

Abstract

Three of six arginine codons (CGU, CGC, and CGA) are decoded by two *Escherichia coli* tRNA Arg isoacceptors. The anticodon stem and loop (ASL) domains of tRNA Arg1 and tRNA Arg2 both contain inosine and 2-methyladenosine modifications at positions 34 (I_{34}) and 37 (I_{34}) and 37 (I_{34}) and 37 (I_{34}). tRNA Arg1 is also modified from cytidine to 2-thiocytidine at position 32 (I_{32}). The I_{32} modification is known to negate webble codon recognition of the rare CGA codon by an unknown mechanism, while still allowing decoding of CGU and CGC. Substitution of I_{32} for I_{32} in the *Saccharomyces cerevisiae* tRNA I_{14} anticodon stem and loop domain (ASL) negates webble decoding of its synonymous A-ending codon, suggesting that this function of I_{32} and I_{32} and I_{33} constructs bound to cognate and webble codons on the ribosome revealed the disruption of a I_{32} constructs bound to failed to fully explain the means by which I_{32} restricts I_{34} webbling. Computational studies revealed that the adoption of a spatially broad inosine-adenosine base pair at the webble position of the codon cannot be maintained simultaneously with the canonical ASL U-turn motif. I_{32} cross-loop interactions are required for stability of the anticodon/codon interaction in the ribosomal A-site.

Introduction

Transfer RNA (tRNA) functions in protein translation by transporting amino acids to the ribosome for protein synthesis. During this process, the tRNA anticodon recognizes and binds the complementary triplet code on messenger RNA (mRNA). The accuracy and efficiency with which tRNA executes this role is significantly enhanced by at least ninety-three currently known naturally occurring posttranscriptional nucleoside modifications, representing a wide array of chemistries and physicochemical properties [1–3]. The most chemically complex and best studied of these modifications occur

within the tRNA anticodon stem and loop (ASL) domain. Among these, modifications to positions 34 and 37, which are respectively within and immediately 3'-adjacent to the anticodon, are the most common [1,4]. The presence of modified nucleosides in the tRNA ASL has been shown to affect its thermal stability and structural conformation [5–10], increase its ribosomal binding affinity [5,6,11–13], enhance specificity of codon decoding [10,11,14–18], maintain the translational reading frame [2,19–21], and promote correct tRNA and mRNA translocation through the ribosome [13]. Modifications have also been demonstrated in some instances to be requirements for

prestructuring the ASL into the canonical tRNA U-turn capable of binding the ribosomal A site [8,10,22-25].

In Escherichia coli (E. coli), six possible mRNA codons specify the amino acid arginine. They are decoded by five different tRNA isoacceptors, each with their own distinct modification profile [4]. Of particular note are the tRNA $^{\rm Arg1}_{\rm \ ICG}$ and tRNA $^{\rm Arg2}_{\rm \ ICG}$ isoacceptors, which share identical ASL primary sequences. The ASLs differ only in one posttranscriptional modification. Only tRNA Arg1 ICG possesses the rare modification 2-thiocytidine (s²C) at position 32, upstream of the anticodon (Fig. 1A). Both ASLs have a 2-methyladenosine at position 37 (m²A₃₇) and an inosine at position 34 (l_{34}) (Fig. 1A and B; Fig. 1D) [26,27]. Outside of the ASL region, tRNA $^{\rm Arg2}$ also possesses an additional nucleoside, A20, in its dihydrouridine loop [4,26,27]. A₂₀, which is present in the other three *E. coli* tRNA Arg isoacceptors as well, has been implicated as an essential aminoacylation determinant [4,26-28]; its deletion or mutation in tRNA Arg2 results in a 370-fold decrease in aminoacylation activity, suggesting that constitutively, tRNA Arg1 is likely to be aminoacylated at a lower efficiency than tRNA Arg2 [29]. It is also possible that A20 in tRNA Arg2 may be an antideterminer with regard to the biosynthesis of s²C₃₂.

The rare 2-thiocytidine modification at position 32 of tRNA Arg1 merits special attention, as the implications of

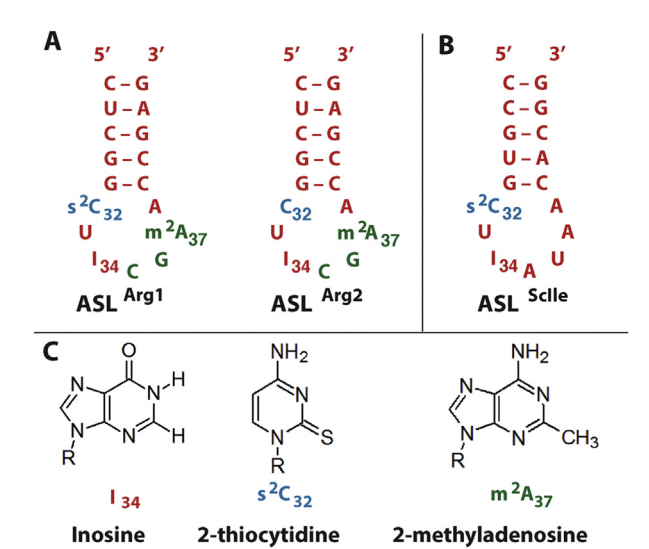


Fig. 1. Anticodon stem and loop (ASL) domain constructs. (A). The primary sequences, secondary structures, and sites of modifications of the constructs for *E. coli* ASL $^{\rm Arg1}$ and ASL $^{\rm Arg2}$. (B). The primary sequence, secondary structure, and sites of modifications of *S. cerevisiae* ASL $^{\rm Ile}$. *S. cerevisiae* tRNA $^{\rm Ile}$ has the modification I $_{\rm 34}$ but C $_{\rm 32}$ is not naturally modified. The s 2 C $_{\rm 32}$ (blue) was introduced into two of the ASL $^{\rm Ile}$ constructs under investigation. (C). The atomic structures of the modified nucleosides inosine (I), 2-thiocytidine (s 2 C), and 2-methyladenosine (m 2 A).

this unusual cytidine thiolation are only just beginning to be explored [1,30,31]. Although s²C is observed in species in both the Archaea and Bacteria kingdoms, it occurs much more rarely than other thiolated tRNA nucleosides, such as the relatively common 2-thiouridine at position 34 (s²U₃₄) or methylthioadenosine derivatives at position 37 [32,33]. In E. coli, the s²C modification at position 32 is observed only in the members of the tRNA Arg family (except tRNA Arg2) and in tRNA Ser2 GCU [1,4,34]. In all known instances, s²C₃₂ is found within a common consensus sequence element, C₃₂U₃₃NC₃₅NA₃₇A₃₈ [4,35], characterized by a conserved cytidine at the second position of the anticodon, a modified purine at position 37, an adenosine at position 38, and the invariant U₃₃. The cytidine at position 35 has, such as A20, been shown to be a key determinant for aminoacylation [27-29]. In all known tRNA structures, C32 and A38 interact via a conserved bifurcated hydrogen bond between the O2 of C₃₂ and the N6 of A₃₈ that forms a noncanonical mismatch base pair at the junction between the stem and loop regions of the ASL [36].

Consistent with the predictions of the Wobble Hypothesis, the presence of inosine (a structural analog of guanosine) in wobble position 34 enables tRNA Arg1 ICG and tRNA Arg2 ICG to decode not only their cognate codon CGC but also the wobble codons CGU and CGA [37]. Both *E. coli* and *Saccharomyces cerevisiae* (*S. cerevisiae*) decoding of CGA have been noted to be inherently inefficient in the presence of I₃₄ [38–40]. The roles of the s²C₃₂ and m²A₃₇ modifications in tRNA Arg1 ICG and tRNA Arg2 ICG, however, are only partially understood.

The structural and functional properties of 2-thiocytidine were initially predicted to mimic those observed for the similarly modified pyrimidine 2-thiouridine (s²U), which occupies the wobble position of several tRNA species. The s²U modification has been shown to increase the degree of base stacking between U₃₄ and U₃₅ [41], an effect attributed to the greater polarizability of sulfur in comparison to oxygen [42,43]. The larger van der Waals radius of sulfur also significantly promotes the adoption of a C3'-endo sugar pucker and an *anti*-conformation of the N-glycosidic (X) dihedral angle in both U₃₄ and its 3'-neighbor at position 35 [14,44—46].

Given that precedent and with the observation that a change from C_{32} to s^2C_{32} alters the accessibility of the tRNA ^{Arg1} anticodon loop to nuclease S1 in a pattern more indicative of an initiator tRNA than an elongator [47], it seemed that the structure or conformation of the stacked bases at positions 31, 32, and 33 in the canonical U-turn of tRNA ^{Arg1} might be altered in the presence of s^2C_{32} . The less electronegative sulfur was also predicted to disrupt the conserved C_{32} - A_{38} cross-loop base pair, a stable interaction known to affect the conformation of the ASL domain [36,41,48]. However, although the presence of s^2C_{32} in *E. coli* ASL ^{Arg1} lCG was shown

spectroscopically to decrease thermodynamic stability and increase base stacking of the RNA, nuclear magnetic resonance (NMR) solution structures of variously modified ASL^{Arg1} and ASL^{Arg2}_{ICG} constructs were found to be nearly identical. Unusually, they were all observed to adopt a 5'-UNCG-3' tetraloop conformation in solution rather than the expected prestructured U-turn motif [14].

In this study, we describe the mechanism by which the 2-thiocytidine modification at position 32 attenuates wobble recognition of adenosine by inosine. An unrelated yeast ASL was engineered to contain both modifications and demonstrated that the effects observed in modified tRNA Arg1 are not unique to this specific tRNA and may be more universally applicable. To better understand the structural basis of that effect, four crystal structures were solved of variously modified ASLs of E. coli tRNA Arg1 and tRNA Arg2 ICG bound to both cognate and synonymous wobble codons in the ribosomal A site. We compared these structures to a previously published crystal structure of a shorter ASL Arg ICG construct, with only the one modified nucleoside, I_{34} , bound to CGA on the ribosome. This CGA-bound ${\rm ASL}^{\rm Arg}{}_{\rm ICG}$ construct revealed a significant displacement of the C₃₂ nucleobase, disrupting the classic bifurcated crossloop C₃₂-A₃₈ hydrogen bond. This suggested the C₃₂-A₃₈ interaction as a structural locus that might be further disrupted upon s²C₃₂ modification. Indeed, previous studies have pointed to other systems in which modification, or changes to the identity, of the nucleoside occupying position 32 (resulting in a weakened interaction between 32 and 38) has had an effect on local conformational flexibility, ribosomal A site affinity, and translational fidelity [36,49-51]. Accordingly, molecular dynamics (MD) simulations were used to model the ribosome-bound structures of various modified ASL Arg1 and ASL Arg2 constructs and mRNA codons. Results indicated that the addition of the sulfur moiety of s²C₃₂ disrupts the ability of the purine inosine to wobble pair with another purine at the anticodon-codon interface because of stress imparted to the structure by the adoption of a distorted C₃₂-A₃₈ cross-loop hydrogen bond. This altered intraloop interaction sterically hinders formation of the canonical U-turn motif and thus, tRNA Arg1 insertion into the ribosomal A site, thereby abolishing CGA, but not CGU or CGC, codon binding.

Results

Thermodynamic and conformational properties of $\rm s^2C_{32}$ and $\rm I_{34}$ in the ASL are consistent across tRNAs

Previous studies [14] suggested thermodynamic, conformational, and functional consequences of

the combined presence of 2-thiocytidine at position 32 and inosine at position 34 of the tRNA Arg1 and tRNA Arg2 isoacceptors. To assess those effects in other molecular contexts, four ASL constructs of 5base pair stems and 7-membered loops of S. cerevisiae tRNA IIe IAU were designed to contain various possible combinations of s 2 C $_{32}$ and I $_{34}$: ASL $^{IIe}_{AAU}$ with and without s 2 C $_{32}$ and ASL $^{IIe}_{IAU}$ with and without s²C₃₂. The ASL of S. cerevisiae tRNAle lau was chosen to test our hypothesis that the C_{32} - A_{38} cross-loop interaction plays a critical role in s^2C_{32} -dependent codon restriction because in addition to naturally occurring I₃₄, it contains an unmodified C₃₂ that participates in a canonical C₃₂-A₃₈ interaction. Furthermore, the second and third anticodon positions differ from E. coli ASLArg1 (Fig. 1A and B) [4]. If our hypothesis regarding s²C₃₂-dependent wobble restriction is correct and does not rely on ASL features other than s^2C_{32} , I_{34} , and a C_{32} - A_{38} cross-loop interaction, ASL ^{III} with an s²C₃₂ modification will bind NNU and NNC codons only (not NNA). *S. cerevisiae* ^{Ile} _{IAU 34} [4] Standard phosphoramidite and 5'-silyl-2'-acetoxyethyl orthoester (ACE) [52] chemistries were used to synthesize the four differently modified ASL $^{\rm lle}$ constructs: ASL $^{\rm lle}$ AAU, ASL $^{\rm lle}$ AAU; s $^{\rm 2}$ C32, ASL $^{\rm lle}$ AAU, and ASL $^{\rm lle}$ AAU; s $^{\rm 2}$ C32 (Fig. 1C) [53].

The thermodynamic and conformational properties of the modifications to the ASL lie were assessed using UV-monitored thermal denaturation studies and circular dichroism (CD) spectroscopy (Fig. 2A and B). In agreement with trends observed previously for modified ASLArg, the addition of either inosine or 2-thiocytidine to ASL IIe resulted in a modest and reproducible reduction in thermal stability (Table 1) [14]. The introduction of 2thiocytidine at position 32 (s²C₃₂) to ASL^{III} AAU also lowered the melt temperature (T_m, the temperature at which half of the ASL hairpins are fully denatured) by 7.2 C compared with that of the unmodified ASL^{lle} AAU and resulted in an increase in the Gibbs free energy at 37 C ($\Delta\Delta G_{37}=-1.96$ kcal/mol). The magnitude of this effect on melting temperature and overall stability agrees well with that observed upon addition of s²C₃₂ to unmodified ASL^{Arg}_{ACG} [14]. A destabilization of similar magnitude was observed upon the addition of an inosine at position 34 (I_{34}) to the unmodified ASL; the T_m decreased by 6.1 °C, whereas the $\Delta\Delta G_{37}$ increased by 1.81 kcal/mol. The doubly modified ASL $^{lle}_{lCG}$:s $^2C_{32}$ construct showed the most dramatic decrease in thermodynamic stability and suggested a modest additive destabilizing effect of the two modifications ($\Delta T_m = 7.8$ °C; $\Delta\Delta G_{37} = -2.39$ kcal/mol). These trends differed only slightly from those observed for the E. coli ASLArg constructs for which similar increases in Gibbs free energy were noted for the singly and doubly modified ASLs but in which the introduction of inosine by itself had no significant effect on melting temperature [14].

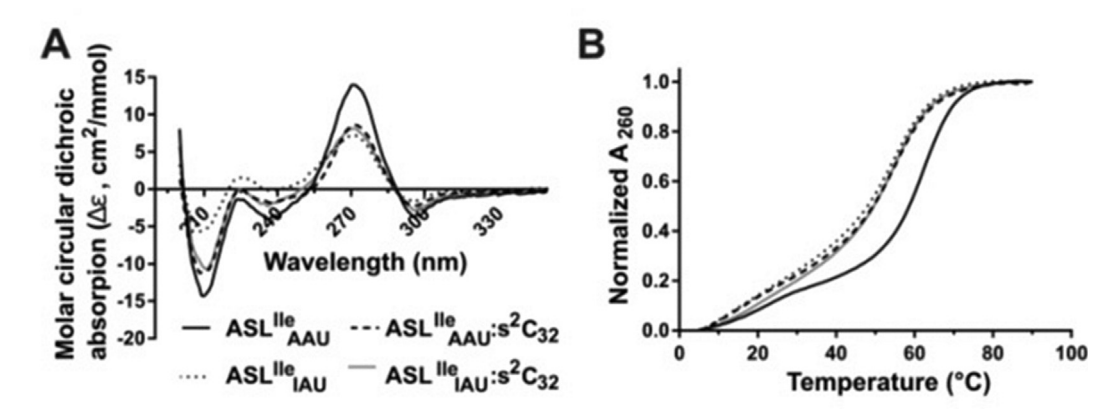


Fig. 2. Thermal stability and base stacking of the *S. cerevisiae* ASL ^{lle} constructs. (A). Circular dichroism (CD) spectra of the four ASL ^{lle} constructs. Spectra are the averages of six normalized molar circular dichroic absorption spectra with data points collected at a resolution of 1 nm. (B) UV-monitored thermal denaturation and renaturation spectra of the ASL ^{lle} constructs (1 mL; ~0.2 OD₂₆₀) collected at 260 nm. The profiles shown are the first derivative plots of the averages of four repeated denaturation/renaturation cycles (5–95 °C; 1 °C/min). ASL, anticodon stem and loop.

Table 1. Thermal stability and properties a of the four ASL le constructs.

ASL ^{IIe}	Δ H (kcal/mol)	ΔS (cal/K*mol)	Δ G (kcal/mol, 37 °C)	T _m (°C)	Hyperchromicity (%)
ACG ACG-s ² C ₃₂ ICG ICG-s ² C ₃₂	-53.7 ± 0.6 -38.0 ± 8.3 -38.7 ± 0.4 -32.1 ± 3.1	-159.7 ± 1.1 -115.3 ± 24.9 -117.0 ± 22.1 -97.6 ± 9.3	$\begin{array}{c} -4.18 \pm 0.02 \\ -2.22 \pm 0.59 \\ -2.37 \pm 0.55 \\ -1.79 \pm 0.19 \end{array}$	63.2 ± 0.2 56.1 ± 0.9 57.1 ± 0.8 55.4 ± 0.3	35.4 ± 1.2 27.6 ± 1.7 27.4 ± 0.9 26.8 ± 1.3

ASL, anticodon stem and loop.

Two experimental values are often consulted to give insight into base stacking within a nucleic acid construct and to identify the changes that occur upon introduction of modified nucleosides: the change in hyperchromicity observed during thermal denaturation and the ellipticity calculated by CD spectroscopy [2,20]. The CD spectra of all four ASL constructs exhibited positive ellipticity ($\Delta \varepsilon$) between 250 and 290 nm ($\lambda_{max} \approx 270$ nm), a hallmark of A-form RNA (Fig. 2A) that also decreased upon introduction of either modification singly or together. The magnitude of the change was similar for all modification states, and this decrease in ellipticity, consistent with the observed changes in hyperchromicity, also suggested a decrease in base stacking. The introduction of $\rm s^2C_{32}$ or $\rm I_{34}$ singly or simultaneously to S. cerevisiae ASL $^{\rm Ile}_{\rm AAU}$ caused a significant reduction of ~8% in observed hyperchromicity relative to that of the unmodified ASL, suggesting a decrease in base stacking (Fig. 2B). These results agree well with previous studies that reported that modifications to the 5' side of the ASL, such as those at or upstream of wobble position 34, tend to disorder and destabilize the structure [24,43]. They also mirror the reported effect of inosine on base stacking in the

ASL^{Arg} constructs, although the effect of s²C₃₂ is significantly more pronounced in *S. cerevisiae* ASL^{IIe}, perhaps an effect of the local chemical environment [14].

The s²C₃₂-mediated restriction of tRNA wobble decoding is a functional property observable in other tRNA species

The striking discovery that the introduction of 2-thiocytidine at position 32 in $E.\ coli$ tRNA $^{Arg1}_{ICG}$ acts to restrict its ability to wobble decode its noncognate CGA codon (yet still correctly reading CGC and CGU) led to the exploration, in this study, of the effect of the presence of an s^2C_{32} on the ability of other tRNAs to recognize adenine in the third codon position. $S.\ cerevisiae$ tRNA $^{Ile}_{IAU}$, such as $E.\ coli$ tRNA Arg2 , contains native C_{32} , I_{34} , and A_{38} nucleosides but otherwise contains neither an endogenous s^2C_{32} modification nor any other sequence homology to tRNA Arg1 or tRNA Arg2 . To investigate the functional effect of s^2C_{32} , ribosome A-site binding of $S.\ cerevisiae$ ASL $^{Ile}_{IAU}$ and ASL $^{Ile}_{IAU}$: s^2C_{32} was assessed *in vitro* to its cognate (AUC) and synonymous wobble codons (AUU and AUA) using 70S

^a Determined from curve-fitting analysis of thermal denaturation curves using MeltWin, v3.5. All errors are reported as standard error of the mean.

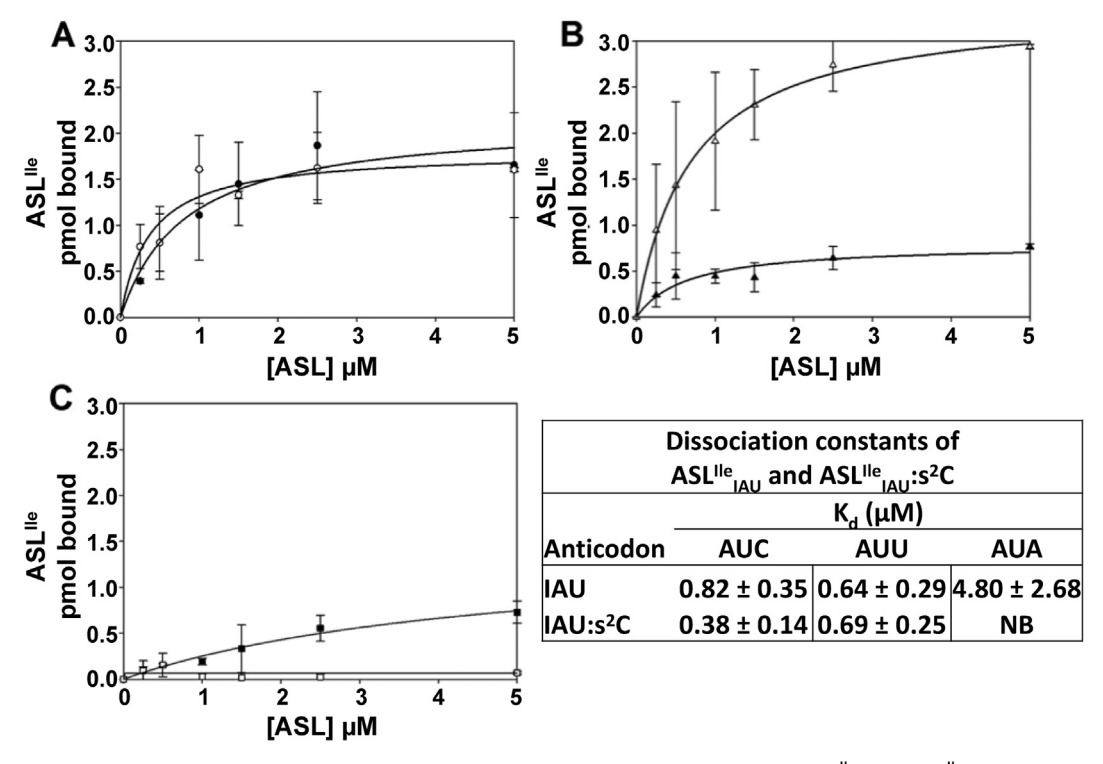


Fig. 3. Ribosomal A site codon binding by modified and unmodified *S. cerevisiae* ASL $^{\text{Ile}}_{\text{IAU}}$. ASL $^{\text{Ile}}_{\text{IAU}}$ (open symbols; \circ $_{\triangle}$ $_{\square}$) and ASL $^{\text{Ile}}_{\text{IAU}}$:s 2 C $_{32}$ (filled symbols; \bullet $_{\blacksquare}$) bound in the ribosomal A site to mRNA codons (A). AUC, (B) AUU, and (C) AUA. Error bars represent standard error of the mean. Table shows dissociation constants (K_d) derived from ribosomal A site codon binding assays and calculated from a one-site saturation ligand binding model in SigmaPlot, version 13.0 (Systat Software, San Jose, CA). "NB" indicates no measurable binding above background. ASL, anticodon stem and loop.

 $E.\ coli$ ribosome binding assays. Consistent with the predictions of the wobble hypothesis for ASLs with inosine in position 34 [37], ASL $^{\rm lle}_{\rm IAU}$ bound to its cognate AUC codon and to AUU and AUA, with physiologically relevant binding constants (Fig. 3A–C; Fig. 3 table inset). The addition of the 2-thiocytidine modification at position 32, however, completely abrogated binding of the S. cerevisiae ASL $^{\rm lle}_{\rm IAU}$:s 2 C $_{32}$ to the noncognate codon AUA. This negative function for the s 2 C $_{32}$ modification, in which it restricts the expected wobble decoding of inosine of codons ending in adenine, is identical to that observed in ribosomal A site binding assays of E. coli ASL $^{\rm Arg1}_{\rm ICG}$:s 2 C $_{32}$ to CGA [14].

X-ray crystallographic structures of modified E. coli ASL Arg1 ICG and ASL Arg2 ICG constructs bound to mRNA on the ribosome are nearly identical

The thermodynamic and ribosome binding studies of the *E. coli* ASL^{Arg1}_{ICG} and the ASL^{Arg2}_{ICG} in the context of an *S. cerevisiae* tRNA^{IIe}_{IAU} suggested that the 2-thiocytidine modification in position 32 has a demonstrable effect on the thermodynamic proper-

ties, base stacking, and wobble decoding ability of the ASL region. Recently published NMR solution structures of several ASL Arg1 and ASL Arg2 constructs bearing different combinations of the modifications s²C₃₂, I₃₄, and m²A₃₇, however, were virtually identical and gave few hints as to the structural basis for the functional effect of s²C on inosine wobbling [14]. Interestingly, all four available NMR structures of modified ASL Arg domains adopted noncanonical 5'-UNCG-3' tetraloop conformations, rather than the expected U-turn motif for ribosomal A site binding, although binding studies showed all four ASLs to be competent for ribosomal interaction [14].

To determine whether a structural effect of s²C₃₂ on ASL structure and codon binding might instead become observable in the context of mRNA binding on the ribosome, where the ASL would be expected to have adopted its functional U-turn conformation, four x-ray crystal structures were determined by molecular replacement. Native *Thermus thermophilus* 30S crystals were soaked with solutions containing each of the variously modified ASL Arg constructs and one of two hexameric RNA oligonucleotides (5′-CG(U/C)AAA-3′) (Fig. 4 and Table S2). The four

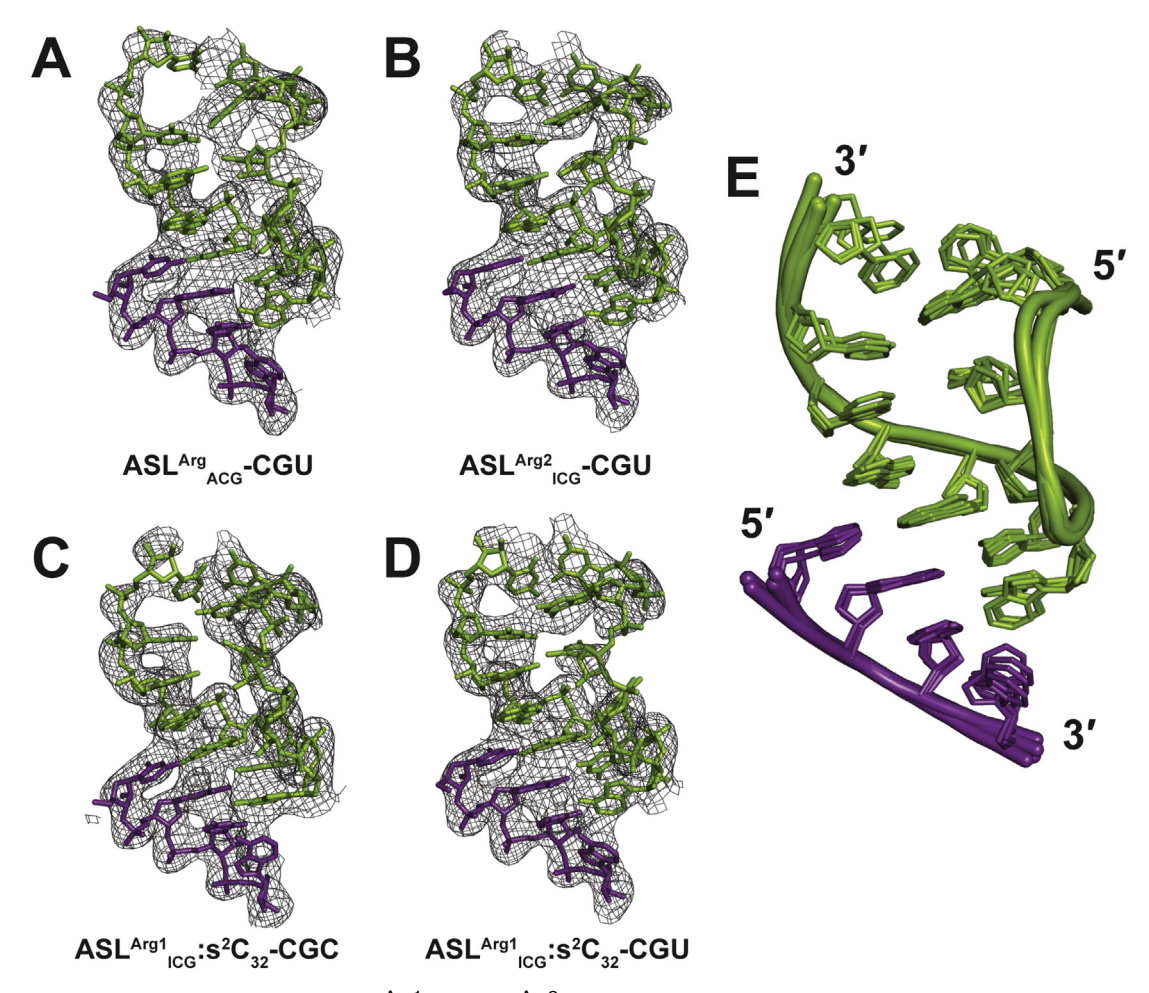


Fig. 4. Crystal structures of *E. coli* ASL^{Arg1} and ASL^{Arg2} constructs on the ribosome responding to the arginine codons CGC and CGU. *E. coli* ASL^{Arg} constructs (green with anticodons) and mRNAs (violet) were soaked into empty cryoprotected *T. thermophilus* 30S ribosome crystals. (A) ASL^{Arg}_{ACG} bound to the arginine codon CGU; (B) ASL^{Arg2}_{ICG} bound to CGU; (C) ASL^{Arg1}_{ICG}:s²C₃₂ bound to CGC; and (D) ASL^{Arg1}_{ICG}:s²C₃₂ bound to CGU. Structures are displayed with 2mFo-DFc maps contoured at sigma = 1.25. (E) Overlay of ASL^{Arg} crystal structures. The interactions of the ASLs with the various mRNA codons for all four structures were aligned using ASL^{Arg}_{ACG} as reference. ASL, anticodon stem and loop.

crystal structures comprise the unmodified ASL Arg ACG with the codon CGU, the ASL Arg2 ICG with CGU, and the ASL Arg1 ICG:s 2 C32 with CGC and CGU. Not unexpectedly, diffraction-quality crystals of an s 2 C32-modified ASL Arg1 ICG in complex with the CGA codon were unattainable. The antibiotic paromomycin was included as an established crystallographic aid in facilitating the formation of the closed form of the 30S subunit; this is known to improve diffraction resolution and result in better ordered electron density for the tRNA moiety [54,55].

The electron density maps are not identical, but no significant differences were observed between the four crystal structures (Fig. S4). Unbiased model refinement resulted in structures having a maximum root-mean-square deviation (RMSD) between all four of the ribosome-bound inosine-containing ASLs with and without the $\rm s^2C_{32}$ modification of

1.09 Å (crystallographic parameters and RMSDs, Tables S2 and S3). Therefore, the small density differences that were observed are likely to be experimental variability. In all four structures, the stem of the ASLArgICG constructs exhibited the geometric features characteristic of an A-form RNA conformation with Watson-Crick base pairs [56]. The structures of the codon-anticodon base pairs are in conventional Watson-Crick or wobble geometry, as expected. The structure of the 30S ribosomal subunit is identical within experimental error to other tRNA-codon recognition ribosome structures published previously [56-58]. The 2-thiocytidine at position 32, when present, caused no discernible perturbation to any structural feature of the ASL compared with structures in which it was absent.

In 2004, Murphy and Ramakrishnan [57] published two related structures, depicting shorter *E. coli*

ASL $^{\rm Arg2}_{\rm ICG}$ constructs (bearing no other modifications) in complex with cognate CGC and noncognate CGA codons on the 30S *E. coli* ribosome. They used these structures as the basis of an experimental demonstration that the wobble inosine-adenosine pair adopts an I_{anti}/A_{anti} geometry at the anticodoncodon interface. When comparing these structures to the crystal structures solved previously, which did not include a CGA-bound structure, a salient point of divergence emerged (Fig. 5A and B). The orientation of the C_{32} nucleobase when ASL $^{\rm Arg2}_{\rm ICG}$ is bound to

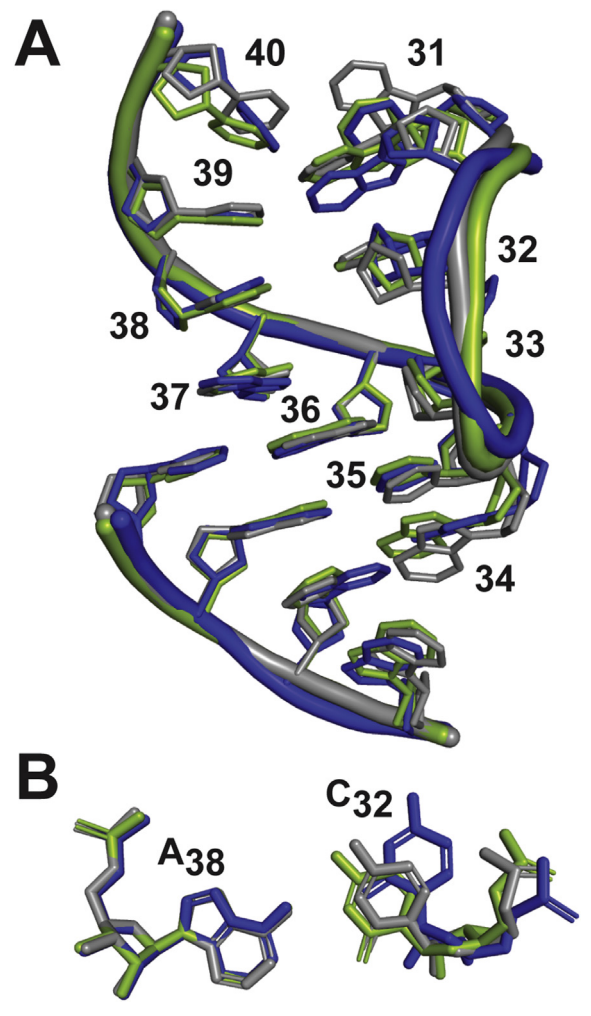


Fig. 5. Comparison of ASL^{Arg} crystal structures with previously solved structures. (A) The ASL^{Arg2}_{ICG} (gray) interaction with the mRNA codon CGU is used as a representative of the structural set and superimposed onto the previously solved structures of the truncated ASL^{Arg2}_{ICG} binding the CGC codon (green) and the CGA codon (blue) [57]). (B) A comparison of the C_{32} - A_{38} base pair with the ASL^{Arg2}_{ICG} construct reveals a deviation in the structure when bound to the rare codon CGA; same coloration as in (A). The structure results from the altered geometry of the I_{34} :A3 anticodon-codon base pair. ASL, anticodon stem and loop.

CGA [57] deviates from the orientation observed when the ASL $^{\rm Arg2}_{\rm ICG}$ instead binds CGU (or CGC). When the backbones of the structures of ASL $^{\rm Arg2}_{\rm ICG}$ bound to the CGA and CGC codons are aligned, the C $_{\rm 32}$ nucleobase can be observed to have rotated by 38° (Fig. 5B). The hallmark hydrogen bonds forming the stable bifurcated C $_{\rm 32}$ -A $_{\rm 38}$ cross-loop interaction are abrogated under inosine-adenosine wobble binding. The amine group on A $_{\rm 38}$ (N6) is within hydrogen bonding distance of N3 on C $_{\rm 32}$ when the codon is CGC (or CGU). When the ASL binds to the CGA codon, the distance between A $_{\rm 38}$ (N6) and C $_{\rm 32}$ (N3) is close to 5 Å, which prevents any direct cross-loop interaction.

It was not possible to obtain a crystal structure of the most interesting ribosome-bound complex, containing an $\rm s^2C_{32}$ -modified ASL $^{\rm Arg1}_{\rm ICG}$ interacting with CGA. This is an anticipated absence, given that no binding was detected between those species experimentally. Having observed, however, that the unmodified $\rm C_{32}$ of ASL $^{\rm Arg2}_{\rm ICG}$ exhibits a conformational distortion when bound to CGA, it was interesting to speculate that the replacement of an oxygen atom with a sulfur atom at that position might compound the effect observed. Because a complex between ASL $^{\rm Arg1}_{\rm ICG}$ -s $^{\rm 2}C_{32}$ and a CGA codon does not form on the ribosome and an x-ray crystal structure could not be obtained, *in silico* MD methods were used to study the effect of 2-thiocytidine on inosine-adenosine binding at the anticodon-codon interface.

Force field parameters developed for the modified nucleoside 2-thiocytidine agree with experimental properties

Force field parameters for MD are readily available for inosine, a common modified nucleoside, but it was necessary to develop and validate a set of novel force field parameters for 2-thiocytidine to simulate s²C-containing RNA molecules accurately. Briefly, AMBER(Assisted Model Building with Energy Refinement) type parameters were developed as described in detail in the Supplementary Materials. Predictions from simulation about the distributions of the syn-anti glycosidic and sugar pucker angles of 2thiocytidine in solution were compared to experimental results obtained by NMR (Figs. S1 and S2) and found to be in good agreement. The difference in the free energy of folding between the ${\sf ASL}^{\sf Arg2}{}_{\sf ICG}$ and ${\sf ASL}^{\sf Arg1}{}_{\sf ICG}{}_{:S}{}^{\sf 2}{\sf C}_{32}$ hairpins determined experimentally by UV-monitored thermal denaturation studies ($\Delta\Delta G_{37} = 0.5 \pm 0.10$ kcal/mol) [57] was also in good agreement with that obtained from simulation using the new $\rm s^2 C$ force field parameters $(\Delta\Delta G_{37}=0.37\pm0.12 \text{ kcal/mol})$ (Fig. S3). These results suggest that the force field parameter set for 2-thiocytidine correctly captured the in vitro behavior of the nucleoside, and it was used in the remainder of the studies reported here.

MD simulations of ASL^{Arg}_{ICG} constructs bound to mRNA on the ribosome indicate that the purine:purine I_{34} - A_3 interaction destabilizes the canonical U-turn motif

To investigate the effects of nucleoside modifications on the structure of tRNA Arg bound to mRNA on the ribosome, simulations were performed for ASL-Arg ICG binding to each synonymous arginine codon (CGC, CGU and CGA) with and without the s2C modification at position 32. Initially, a 10-ns simulation of each of the structures with the entire ribosome intact demonstrated that the system does not exhibit any structural rearrangements, in either the presence or absence of the modification. Expected interaction between the ribosomal subunit and its tRNA and mRNA substrates (specifically between tRNA and mRNA residues and ribosome nucleosides G530, A1492, A1493) are maintained throughout the simulations. Therefore, to simplify the system and permit longer simulations, the system of interest was thereafter defined as composed of the tRNA and mRNA moieties, an intact stable fragment of the ribosomal RNA which includes all residues making direct contacts with the tRNA and/or mRNA, and associated Mg²⁺ ions. All simulations were run for

As predicted by numerous previous structural studies, when ${\rm ASL}^{\rm Arg1}{}_{\rm ICG}$ or ${\rm ASL}^{\rm Arg2}{}_{\rm ICG}$ binds CGC or CGU, the inosine at position 34 of the ASL interacts in standard wobble geometry with the smaller pyrimidine ring (U₃/C₃) of the third nucleoside in the mRNA codon [54,57,59]. The standard C1'-C1' distance between a purine-pyrimidine base pair is in the range of 10.2–10.8 Å [37], a characteristic that can be observed in these MD simulations as well when the mRNA codon is either CGC or CGU. In this conformation the canonical Uturn interaction, in which U₃₃ interacts with the phosphate group of G₃₆, is also maintained, as previously observed in simulations and experimentally obtained structures [60–62].

In the case in which the ASL ^{Arg}_{ICG} binds the CGA codon, however, I₃₄ must form a wobble base pair with the larger purine ring of adenosine (A₃), an interaction which occupies a broader spatial extent [38,57]. To accommodate the larger adenosine in position 3 of the CGA codon, the C1'-C1' distance between I₃₄ and A₃ becomes 2.5 Å greater than the standard purine-pyrimidine distance, occupying nearly 13 Å total [37]. Previous reports based on x-ray crystallography suggested that when ASL ^{Arg2}_{ICG} binds CGA on the ribosome, the ASL absorbs this structural perturbation chiefly through modest changes in torsion angles between the C1 and P atoms of the inosine [57]. Examination of these

simulation results confirmed that those torsion angle alterations occur but also demonstrated that the purine-purine displacement at the wobble position propagates further than I₃₄. This is reflected in a significantly distorted U-turn in which the U₃₃, instead of interacting with the phosphate group of G₃₆ as in a canonical U-turn [60–62], now interacts with C₃₅ through the O2' hydroxyl group (Fig. 6A and B) This altered hydrogen bonding brings about two important changes: (a) it introduces a kink in the ASL domain that results in a rotation of the C_{32} nucleobase away from the center of the loop domain, as also observed experimentally by x-ray crystallography [60-62] and (b) U₃₃ rotates toward the outside, opening the loop cavity for hydration water molecules. In this conformation, the classic bifurcated cross-loop hydrogen bond between C₃₂ and A₃₈ is disrupted (Fig. 6C and D) and is instead replaced by dynamic water-mediated interactions involving the N6 and O2 of the tRNA's A₃₈ and C₃₂ bases, respectively, with one or two bridging water molecules. This behavior is in contrast to the binding of ${\rm ASL}^{\rm Arg2}_{\rm \ ICG}$ to CGC or CGU, in which the wobble position inosine forms a standard Watson-Crick bond with a pyrimidine nucleoside, and N6 of A₃₈ and N3 of C₃₂ participate in the classic bifurcated hydrogen bond. In this confirmation, the oxygen on the second position (O2) of C₃₂ faces away from the interior of the loop domain. When C₃₂ is unmodified and the codon is CGA, it appears clear that the O2 directly participates in maintaining the loop hydrated with at least one dynamic H₂O molecule (Fig. 7 & Supplementary video). The absence of these water molecules in the published crystal structure [57] is not surprising because of their highly dynamic nature (Supplementary video).

Supplementary video related to this article can be found at https://doi.org/10.1016/j.jmb.2019.12.016.

A canonical interaction and structure are obtained when $\mathsf{ASL}^\mathsf{Arg2}$ containing only I_{34} binds CGU or CGC but CGA binding results in a distortion of the U-turn that propagates as far as the C₃₂-A₃₈ crossloop interaction. It therefore seemed probable that the 2-thiocytidine modification at position 32 of ${\rm ASL}^{\rm Arg1}{}_{\rm ICG}{:}{\rm s}^{\rm 2}{\rm C}_{\rm 32}$ would compound the structural instability obtained when a purine-purine interaction occupies the wobble position. Accordingly, the same simulations were performed on the system in which s^2C_{32} replaced C_{32} in silico. A stable interaction does not form naturally between the mRNA CGA codon on the ribosome and the s²C₃₂modified ASLArg1 ICG; thus, the simulation included an extra set of constraints on the ASL itself, holding it fixed in its initial distorted U-turn structure such that the binding interface between codon and anticodon could not be destabilized. In this way, we were able to account for the failure of ASL Arg1 _{ICG}:s²C₃₂ to form a complex with CGA under biological conditions.

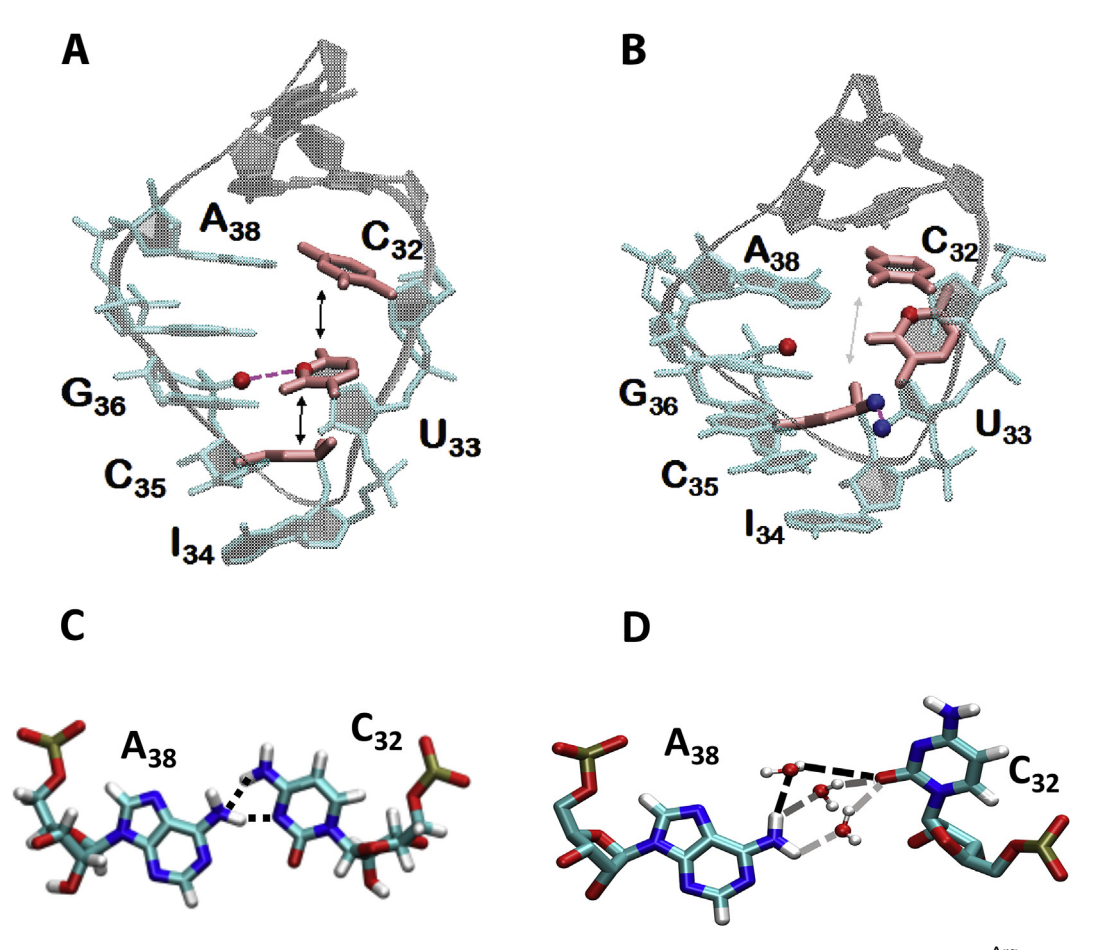


Fig. 6. Molecular dynamics (MD)-simulated comparison of the U-turns and A_{38} - C_{32} interactions in ASL $^{Arg}_{ICG}$ binding the codons CGU (PDB ID: 6MKN) and CGA (PDB ID: 1XNQ). (A) Canonical U-turn with stacking and U_{33} - G_{36} interaction (ASL $^{Arg2}_{ICG}$ bound to codon CGU). (B) Noncanonical U-turn with U_{33} - U_{35} interaction. The stacking interaction and U_{33} - U_{36} interaction are absent (ASL $^{Arg2}_{ICG}$ bound to codon CGA). (C) U_{38} - $U_$

The addition of s^2C_{32} to ASL^{Arg1}_{ICG} had no discernible effect on the structure of the mRNAbound ASL on the ribosome when the bound codon is CGC or CGU and a purine-pyrimidine pair occupies the wobble position. In contrast, when the codon is CGA and the codon-anticodon interaction is enforced, the MD simulations demonstrated that the larger and less electronegative sulfur atom replacing O2 in the s^2C_{32} -modified ASL $^{Arg1}_{ICG}$ is not able to coordinate water and stabilize the water-mediated C₃₂-A₃₈ interaction as efficiently as the oxygen (Supplementary video). The S2-for-O2 substitution is expected to have both enthalpic and entropic penalties. The larger sulfur atom and the longer C=S bond result in a reduction of available space for water molecules inside the loop of the ASL^{Arg1}_{ICG}:s²C₃₂ construct when in complex with CGA, as observed in simulation (Fig. 7). In the presence of s²C₃₂, the water molecules are confined to three distinct clusters, while in the unmodified case the water molecules are relatively dispersed in the

accessible space. The confined, more ordered distribution of water in the presence of the modified s $^2 C_{32}$ implies that the water-mediated interaction occupies a smaller number of possible configurations, resulting in an entropic penalty. The reduced enthalpy arising from the weakened water-mediated interaction and the entropic penalty as a result of the fewer accessible configurations for the water-mediated hydrogen bond between the A_{38} and C_{32} both contribute to destabilization of the loop structure.

Furthermore, in the absence of constraints on the ASL $^{Arg1}_{ICG}$:s $^2C_{32}$ in complex with CGA, the U-turn-stabilizing U_{33} (O2') - C_{35} (OP) hydrogen bond is observed to break, in favor of a U_{33} (O2') - I_{34} (OP) hydrogen bond, further destabilizing the positioning of U_{33} in the loop. While the simulations did not sample the timescales necessary to observe spontaneous unbinding of the ASL from the CGA codon in response to the sulfur modification, they do provide valuable molecular insights into the interactions that

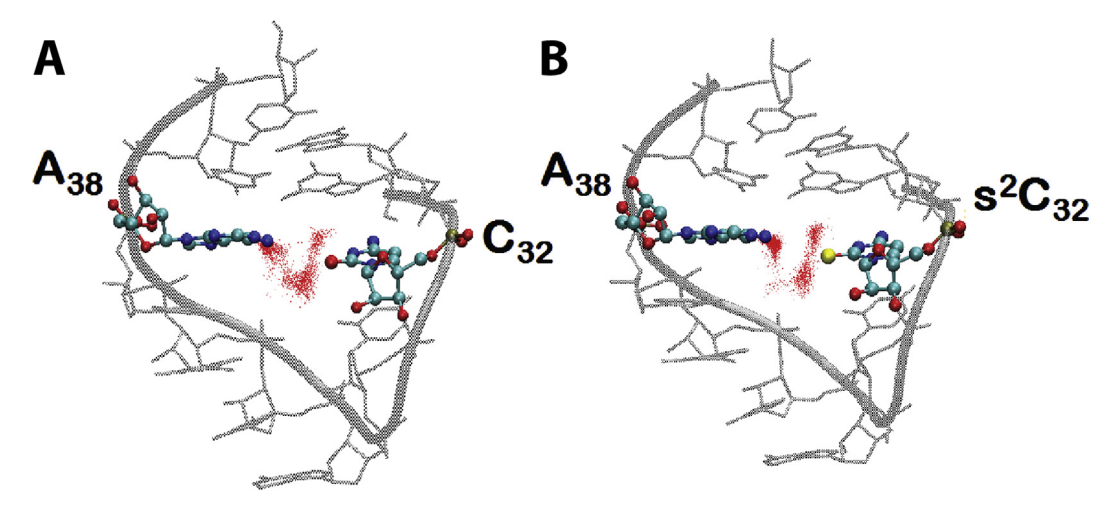


Fig. 7. The MD simulation of the distribution of water inside the loop of the modified ASL^{Arg1}_{ICG} :s $^2C_{32}$ and the ASL^{Arg2}_{ICG} in binding to the codon. The MD simulation was conducted in a water box with 4.3×10^4 water molecules. Each dot represents the oxygen of a water molecule which is within 3.5 Å of the O_2/S_2 of C_{32} and the amine nitrogen, N_6 , of A_{38} , where the water molecule can establish hydrogen bonds with both these groups. Snapshots were recorded every ps. (Supplementary video). ASL, anticodon stem and loop; MD, molecular dynamics.

weaken and finally break. Consequently, they provide insight to the substantial decrease of the experimentally observed binding affinity between tRNA Arg1 ICG:S 2C32 and its cognate codon CGA.

Discussion

The effect of modified nucleosides on the ability of tRNA to recognize codons has been discussed ever since 1966, when Crick published the wobble hypothesis and proposed that an inosine occupying position 34 of the anticodon can bind A, C, or U [37]. Other modifications, particularly those at positions 34 and 37, affect the ASL in a variety of ways, including restricting codon recognition, enabling translocation, prestructuring of the ASL to bind the ribosomal A site in addition to expanding, and restricting wobble recognition [22,58,63]. In fact, the ASL of the two tRNA Arg isoacceptors (tRNA Arg1, tRNA Arg2) discussed here contain another modification at position 37, 2-methyladenosine (m²A₃₇) [1,34]. Aliphatic modifications at position 37 of tRNAs are commonly shown to stabilize the codon-anticodon pairs by additional stacking interactions and thus enhance binding affinity of the tRNA-mRNA complex [1,34]. However, in the case of ASL $^{\rm Arg1}_{\rm ICG}$ and ASL $^{\rm Arg2}_{\rm ICG}$, ribosomal binding studies show that the m²A₃₇ modification also reduces or negates binding of the ASL to its cognate and near cognate codons [14]. A complete structural and dynamic explanation for this counterintuitive result is being pursued using MD simulations and is a part of our ongoing investigative efforts.

Other than s²C₃₂, modifications at position 32 are not uncommon. Modified nucleosides that have been

found at this position include N3-methylcytidine ($\rm m^3C$), 2'-O-methyl-(cytidine, uridine and adenosine) ($\rm Cm$, Um and Am) [64,65] and pseudouridine ($\rm \Psi$). The $\rm m^3C_{32}$ modification has been found to impart resistance to oxidative stress in yeast and higher eukaryotes when present in tRNA Ser and tRNA Thr and in tRNA Arg, respectively [66]. When absent, the lack of $\rm Cm$ at position 32 on tRNA Phe negatively affects translational efficiency of the tRNA [67].

Among the several modifications that occur at position 32; however, the s^2C_{32} modification is rare. The nucleoside s²C was first reported in an E. coli tRNA Ser [68]. An *in vitro* investigation of the synthesis of the T4 phage coat protein in *E. coli* showed that the triply modified tRNA Arg1_{ICG}:s²C₃₂,m²A₃₇ was required to maintain the translational reading frame; substitution of C_{32} for s^2C_{32} increased the incidence of frameshift mutations during translation [47]. A Salmonella enterica mutant unable to synthesize 2thiocytidine exhibited no overall growth disadvantage. but the reintroduction of the modification was observed to decrease the rate of peptide translation for the rare CGA codon and not the common CGU [69]. This finding was in broad agreement with the recent discovery that, while *E. coli* ASL Arg1 _{ICG} (identical to ASL Arg2 _{ICG}) carrying an unmodified C₃₂ binds all three wobble hypothesis—predicted mRNA codons, the s²C₃₂-modified ASL Arg1 _{ICG} was completely unable to bind to CCA although it beauty CCA tely unable to bind to CGA, although it bound CGC and CGU with physiological binding constants [14]. The negative influence of s^2C_{32} on I_{34} decoding of A3 was clearly replicated with a yeast tRNA le ASL construct. Yet, after determining three NMR structures of variously modified ASL constructs of tRNA Arg [14] and four crystal structures of ASLArg1 ICG with and

ASL $^{Arg2}_{\rm ICG}$ without s^2C_{32} on the ribosome in response to various codons, the mechanism by which s^2C_{32} was modulating the ability of I_{34} to read A3 was not clear. A comparison of crystal structures containing the CGU/CGC codon with one containing the CGA codon revealed that in the case of $I_{34}\text{-}A_3$, the hallmark interactions of the canonical U-turn are modified to accommodate the larger purine-purine base pair. This evident structural difference was, however, not itself sufficient to explain the role of s^2C_{32} in negating binding of the ASL $^{Arg1}_{\rm ICG}$:s $^2C_{32}$ to the CGA codon. Taken together, the aforementioned results do suggest both a global role for s^2C_{32} in preventing frameshift mutations during protein translation and a specific role in restricting the ability of tRNA $^{Arg1}_{\rm ICG}$ to decode the rare arginine codon CGA.

MD simulation of the I₃₄-A3 interaction in explicit water appears to have revealed a possible mechanism based on dynamics and the ordering of water by s^2C_{32} between the ASL nucleosides C_{32} and A_{38} . The interaction between the nucleosides Y₃₂-R₃₈ at the base of the loop domain of the ASL is typically characterized by a single or bifurcated hydrogen bond [36]. The strength of this interaction appears to be carefully modulated. While a stronger interaction, similar to that of a canonical base pair, could lead to a loss in flexibility of the loop domain at this position. a weaker interaction could conversely result in loss of stacking between Y_{32} and U_{33} and result in a disruption of the functional U-turn conformation of the ASL. Indeed, the identity of the bases occupying these positions and the nature of their interaction correlates strongly to the affinity of the tRNA for the ribosomal A site for cognate and near cognate codons [51]. The nature of the C₃₂-A₃₈ interaction is attributed to energetic penalties and structural changes that affect the codon-anticodon helix in cognate and near cognate recognition [51]. Thus, we hypothesized that tRNAs having s²C₃₂ have an altered anticodon loop conformation and enthalpy penalties whereas interaction of C₃₂ with A₃₈ could significantly affect wobble of I₃₄ to A3.

In the crystal structure of the ASL Arg2 ICG bound to the CGA codon at the ribosomal A site, the direct cross-loop interaction between C₃₂ to A₃₈ is disrupted in the presence of the I_{34} -A3 interaction [57]. In our MD simulations, we observed that the subtle distortion reported at the codon-anticodon mini-helix of ASL-Arg2 f_{ICG} due to the I_{34} -A3 purine-purine base pair results in a substantially distorted, noncanonical Uturn upstream. This, in turn opens up the loop domain for hydration waters and brings about a watermediated interaction between C₃₂ to A₃₈ involving the O2 atom of C_{32} . It is well established that pseudouridine at position 32 uses a water-mediated base-backbone interaction to stabilize the 32-38 interaction pair [36]. Replacing C₃₂ with s²C₃₂ in the ASLArg1 ICG construct weakens the water-mediated interaction, due to the larger size and weaker electronegativity of the sulfur atom. We hypothesize that this diminished interaction makes formation of the required noncanonical U-turn less favorable, which destabilizes the interactions within the loop and with the mRNA and leads to the inability of $\rm s^2C_{32}\text{-}modified}$ ASL $^{\rm Arg1}_{\rm ICG}$ to bind to the CGA codon.

It is interesting to note that the rare modification s^2C_{32} affects the decoding capacity of the ASL Arg1 $_{ICG}$ only in the case of the similarly rare codon CGA. It does not significantly affect the structure or the ribosomal binding capacity of the ASL Arg1 $_{ICG}$ to the more common CGU and CGC codons of arginine, nor does its absence affect the growth rate or physiology, under laboratory conditions, of bacteria in which it is native [69]. This observation permits speculation that the incorporation of the s^2C_{32} modification in tRNA Arg1 $_{ICG}$ may have originally been an evolutionary accident but that its negative effect on the already inefficient decoding of the rare codon CGA conferred an advantage in some environments.

It is increasingly acknowledged that tRNA modification profiles can be reprogrammed, under various stresses and during environmental changes, to better read specific codons over their synonymous counterparts [70-72]. The reprogramming of tRNA wobble modifications has already been shown to lead to enhanced translation of codon-biased mRNAs (known as modification-tunable transcripts, or MoTTs) with roles in survival and stress response [72,73]. It is not difficult to imagine a similar tunable role for s²C₃₂ in regulating the translation of MoTTs containing disproportionate stretches of rare CGA codons, which have been shown in both E. coli and S. cerevisiae to promote ribosomal stalling and affect translation negatively under ordinary cellular conditions [70,74,75]. An investigation of proteins consisting of a generous percentage of arginines coded by CGA codons and their functions in the bacteria would be useful in understanding the physiological impact of this modification [76].

Material and Methods

Oligonucleotide preparation

The modified nucleoside 2-thiocytidine (s²C) was synthesized chemically (Trilink Biotechnologies, San Diego, CA) and then derivatized to the 5'-Q-BzH-2'-Q-ACE-protected 2-thiouridine-3'-(methyl-N,N-diisopropyl) phosphoramidite (Dharmacon Products; Thermo Fisher, Lafayette, CO). The chemically synthesized heptadecameric *E. coli* ASL^{Arg1} [4] and *S. cerevisiae* ASL^{III} constructs [4,77] were also produced by ACE chemistry [52] to contain A₃₄ or I₃₄ with or without s²C₃₂ (Dharmacon Products; Thermo Fisher). After deprotection via standard protocol, the RNA was desalted and dialyzed against water

using a 3500 Da cutoff membrane (Pierce) followed by resuspension in 20 mM sodium phosphate buffer, pH 6.8.

UV-monitored thermal denaturation and CD

ASLIIe ANA samples (Fig. 1C) were prepared as aforementioned at concentrations adjusted to ~0.3 absorbance units at 260 nm. Thermal denaturations and renaturations were monitored by UV absorbance at 260 nm with a Carv 100 UV-visible spectrophotometer (Agilent) using Thermal software. Five successive denaturations and renaturations were conducted over a temperature range of 5-95 °C using 1-cm pathlength cuvettes. The temperature ramp rate was 1.0 C/min with a data sampling interval of 1 min. Thermodynamic parameters were obtained by fitting absorbance versus temperature profiles using the curve-fitting program Meltwin (version 3.5). After normalization, the first derivative was determined and smoothed by cubic splines. CD spectra on each sample were collected immediately after thermal denaturation studies as a series of six scans on a Jasco 600 spectropolarimeter (Jasco, Inc.) at 20°C in a 1-cm pathlength quartz cuvette. All data were baseline corrected using a control containing buffer only. Data were analyzed by normalizing the spectra to molar circular dichroic absorbance using simultaneously collected absorbance data to calculate the concentrations of each sample $(\Delta \varepsilon = \theta/32980 \cdot C \cdot L \cdot N)$ [78].

Codon-specific ribosomal binding assays

E. coli 70S ribosomes were purified from *E. coli* MRE 600 cultures and used in codon-specific ribosomal A site binding assays as described previously [14]. Together with ASL lle laU constructs, the following mRNA sequences based on the T4 gp32 message and *S. cerevisiae* tRNA-lle laU were used. (A-site codon sequences are bold and underlined.):

- (1) GGCAAGGAGGUAAAAAUGAUCGCACGU
- (2) GGCAAGGAGGUAAAAAUG**AUU**GCACGU
- (3) GGCAAGGAGGUAAAAAUG<u>AUA</u>GCACGU

Heptadecamer ASLs were 5'-32P-radiolabeled and purified using preparative denaturing 15% polyacrylamide gel electrophoresis. mRNA-programmed ribosomes (250 nM ribosome and 2.5 μ M mRNA) were P-site saturated with tRNA fMet and incubated for 1 h at 37°C with varying concentrations (0, 0.25, 0.5, 1.0, 1.5, 2.5, 5 μM) of unlabeled ASL spiked with up to 2 kCPM radiolabeled ASL in ribosome binding buffer (50 mM HEPES, pH 7; 30 mM KCl; 70 mM NH₄Cl; 1 mM DTT; 100 μM EDTA; 20 mM MgCl₂ adjusted to pH 7 with 2 M NaOH). Binding reactions were then filtered through a 0.22 µM nitrocellulose filter (Whatman) using a modified micro-sample filtration manifold (Whatman Schleicher & Schuell Minifold) 96-well dot blot apparatus [79,80]. A standard curve was generated by spotting known amounts of radiolabeled ASL onto a small strip of nitrocellulose filter. Filters were imaged using a Typhoon phosphorimager (GE Healthcare), and radioactive spot density was

calculated using ImageQuant TL software (Amersham). Binding constants were calculated using the onesite—specific binding function in Prism v3 (Graphpad). An internal positive control using unmodified yeast ASL Phe binding to polyuridylic acid and nonspecific negative controls using a control mRNA with GCG in the A-site position were performed in tandem with every experiment. All binding curves were performed in triplicate in each of three independent experiments. Determination of ribosome activity and usability of mRNAs was accomplished using filter binding assays consisting of only ribosomes and 5'-32P-radiolabeled mRNAs. This approach to assessing the binding of tRNA to ribosomes by treating it in the manner of a standard ligand-binding experiment has historical precedents as far back as 1966 [81] and also appears in a large number of more modern studies of ribosome/tRNA interaction [82-84].

Crystallization

Chemically synthesized hexamer mRNA oligonucleotides (5'-CG(U/C)AAA-3') were purified by preparative polyacrylamide electrophoresis (Thermo Fisher Scientific). The 30S ribosome subunits were purified from T. thermophilus followed by crystallization and cryoprotection in 26% (v/v) MPD, 100 mM K-MES (pH 6.5), 75 mM NH₄Cl. 200 mM KCl. and 15 mM MgCl₂ as described [85]. Empty, cryoprotected 30S ribosome crystals were then soaked in cryoprotection solution containing 80 µM paromomycin, 300 μM ASL, and 300 μM mRNA [54,55]. After soaking for at least 48 h. crystals were plunged in liquid nitrogen and stored until data collection. Paromomycin, an antibiotic, induces a closed conformation of the 30S ribosomal subunit without affecting the conformation of the A-site tRNA [55], resulting in improved density and resolution of the ASL [54].

Data collection and refinement

Native RNA-bound ribosome diffraction data were collected at NE-CAT beamlines 24-ID-C and 24-ID-E of the advanced photon source and processed using X-ray Detector Software, XDS [86]. Phases were obtained by molecular replacement using PHENIX with PDB ID: 1XNR a search model [87]. The model was refined in PHENIX, followed by additional refinement, visualization, and model building in Coot [87,88]. The molecular visualizaion system, PyMOL was used for figure production [89]. The eLBOW module within PHENIX was used to generate geometry restraints and dictionary files for the nonstandard residues (paromomycin, inosine, 2-methyladenosine, and 2-thiocytidine) using the semiempirical quantum mechanical AM1 method [90]. Data sets were not collected at the same time; differences in resolution of the structures were, therefore, likely caused by variation in the X-ray beam rather than in the crystals themselves. A summary of data and refinement statistics is given in Table S1. The atomic coordinates for the ASL Arg1 and ASL Arg2 constructs bound to mRNA on the 30S ribosome were deposited in the Protein Data Bank under the accession numbers 6DTI (unmodified ASL^{Arg}_{ACG} binding codon CGU), 6MKN (ASL Arg2_{ICG} binding codon CGU), 6MPF (ASL^{Arg1}_{ICG}:s²C₃₂ binding CGC), and 6MPI (ASL^{Arg1}_{ICG}:s²C₃₂ binding CGU).

Simulation Methods

Force field parameterization and validation

AMBER-type force field parameters for the modified nucleoside 2-thiocytidine (s²C) were obtained and validated as described in detail in the Supplementary Materials. Briefly, published values were used for the partial charges of the s²C atoms, while AMBER-99 force field parameters and AMBER-99 parameters with the Chen-Garcia correction were used for bonded and Lennard-Jones (LJ) interactions, respectively [91,92]. To validate these force field parameters, two sets of MD simulations were performed: (i) single nucleoside simulations of cytidine and 2-thiocytidine and (ii) simulations in solution of ${\sf ASL}^{\sf Arg1}{}_{\sf ICG}$ with the 2-thiocytidine modification at position 32 and of ${\sf ASL}^{\sf Arg2}{}_{\sf ICG}$ without the ${\sf s^2C_{32}}.$ The simulated distributions of the syn-anti glycosidic and sugar pucker angles for s²C in solution were then compared with experimental results obtained from NMR ¹H-¹H nuclear overhauser enhancement spectroscopy-heteronuclear single quantum coherence, and correlation spectroscopy-double quantum filtered (NOESY-HSQC and DQF-COSY)spectra (Figs. S1A and B), and the folding free energy difference between the ASL^{Arg2}_{ICG} and ASL-Arg1_{ICG}:s²C₃₂ RNA hairpins (Fig. S2; Table S1) was compared with that determined experimentally by UVmonitored thermal denaturation studies [14]. The simulation results were in good agreement with experiment, suggesting that the force field parameter set for 2thiocytidine correctly captured the in vitro behavior of the nucleoside.

MD simulations

The crystal structures of the 16S ribosomal subunit of *T. thermophilus* containing the ASL domains of tRNA-Arg1 _{ICG} and tRNA Arg2 _{ICG} and the mRNA codon fragment in the decoding center were obtained from the Protein Data Bank: ASL Arg2 _{ICG} bound to CGC (1XNR) and CGA (1XNQ) [57] or acquired crystallographically as aforementioned: unmodified ASL Arg2 _{ICG} bound to CGU (deposited as 6MKN), ASL Arg1 _{ICG} bound to CGU (deposited as 6MKN), ASL Arg1 _{ICG}:s2C32 bound to CGU (deposited as 6MPF), and ASL Arg1 _{ICG}:s2C32 bound to CGU (deposited as 6MPI). To model the binding of ASL Arg1 _{ICG}:s2C32 to the CGA codon, the cytosine at position 32 in the ASL Arg2 _{ICG}-CGA crystal structure (1XNQ) was modified to s2C32 in silico. Missing atoms and ions in the ribosome-associated proteins were added using MOE [93].

A 10-ns all-atom simulation of each of the structures with the entire ribosome intact was used to demonstrate that the system does not exhibit any changes in the interaction between the canonical tRNA-mRNA pair and the ribosomal subunit. Thereafter, the simulation system included the tRNA and mRNA moieties, an intact stable fragment of the ribosomal RNA comprising those residues making direct contacts with the tRNA and/or mRNA, and associated $\rm Mg^{2+}$ ions in a solution of 1 M KCl in a 3D periodic box. The box size was 11.25 \times 11.25 \times 11.25 nm³ containing ~997 K+ ions, ~884 Cl- ions and 4.3 \times 104 water molecules.

MD simulations were performed using Gromacs-4.6.3 and Gromacs-5.0.6 packages [94]. The MD simulations incorporated a leap-frog algorithm with a 2-fs timestep to integrate the equations of motion. The system was maintained at 300 K, using the velocity rescaling thermostat [95]. The pressure was maintained at 1 atm using the Berendsen barostat for equilibration [96,97]. The longrange electrostatic interactions were calculated using particle mesh Ewald algorithm with a real space cut-off of 1.0 nm [98]. Lennard-Jones interactions were also truncated at 1.0 nm. The TIP3P model was used represent water molecules, and the LINCS algorithm was used to constrain the motion of hydrogen atoms bonded to heavy atom [99]. The system was subjected to energy minimization to prevent any overlap of atoms, followed by 0.5 ns of equilibration in constant pressure-constant temperature ensemble ensemble and a 50-ns constant volumeconstant temperature ensemble production run. During simulations, the ribosomal subunit was held in place using position restraints on its heavy atoms with a force constant of 1000 N/nm in each spatial dimension for the equilibration run and then was frozen for the rest of the simulation. When modeling the binding of ASL^{Arg1}_{ICG}:s²C₃₂ to the CGA codon, the atoms comprising the ASL were held fixed in the conformation adopted during the simulation of the binding of ASL Arg2 ICG without s²C₃₂ to enforce the binding interface between the anticodon and the codon. Coordinates of the RNA components (rRNA, tRNA, and mRNA) of the system were stored every 1 ps for further analysis.

Accession Numbers

The final model coordinates and the corresponding structure factors were submitted to Protein Data Bank with the accession numbers PDB ID: 6DTI (unmodified ASL $^{\rm Arg}$ bound to CGU); PDB ID: 6MNK (ASL $^{\rm Arg2}$ lCG bound to CGU); PDB ID 6MPF (ASL $^{\rm Arg1}$ lCG:s 2 C32 bound to CGC); and 6MPI (ASL $^{\rm Arg1}$ lCG:s 2 C32 bound to CGU).

Acknowledgments

The authors thank Jennifer Lorenz Badua and Thomas Sarachan for assistance in preparing figures.

This work was supported by the National Institutes of Health, National Institute of General Medical Science [2RO1GM23037-25 to P.F.A. and 1R01GM110588-01 to P.F.A. as coinvestigator, Manal Swairjo, Principal Investigator]; and the National Science Foundation [MCB1101859 and CHE1407042] to P.F.A]. H.D. acknowledges support from NSF Science and Technology 349 Centers grant NSF-1231306 (Biology with X-ray Lasers, BioXFEL). The open access publication charge for this article was paid in part from the funding sources aforementioned.

Author contributions

S.V., W.A.C., J.L.S., H.D., F.V.M., S.V.R., and K.L.S. contributed to conducting of the empirical and *in silico* experiments, analysis of data, and feedback on the manuscript; W.A.C. and K.L.S. contributed to writing; and P.F.A. contributed to concept of study, aid in preparation of figures, editing the manuscript and supplementary figures.

Conflict of interest statement

No conflict of interest exists with any of the authors.

Appendix A. Supplementary data

Supplementary data to this article can be found online at https://doi.org/10.1016/j.jmb.2019.12.016.

Received 3 May 2019; Received in revised form 25 November 2019; Accepted 5 December 2019 Available online 14 January 2020

Keywords:

RNA structure; RNA function; tRNA; modified nucleosides; wobble decoding

[†]These authors contributed equally to the paper as first

[‡]Present address: Paul F. Agris, Department of Medicine, Duke University Medical School, Durham, NC, 27710, USA.

[§]Department of Chemistry and Biochemistry, Ohio State University, Columbus, OH 43210 USA.

Division of Integrated Sciences, Wilson College, Chambersburg, PA 17201 USA.

[¶]BIO-CAT Microbials, Shakopee, MN 55379 USA. [#]The RNA Institute, 1400 Washington Avenue, Albany, NY 12222 USA.

Abbreviations used:

tRNA, transfer RNA; mRNA, messenger RNA; ASL, anticodon stem and loop; s²C, 2-thiocytidine; m²A, 2-methyladenosine; I, inosine; s²U, 2-thiouridine; MD, molecular dynamics; NMR, nuclear magnetic resonance; MoTTs, modification-tunable transcripts; ACE, 5'-silyl-2'-acetoxyethyl orthoester; CD, circular dichroism; NOESY-HSQC, nuclear overhauser enhancement spectroscopy-heteronuclear single quantum coherence; COSY-DQF, correlation spectroscopy-double quantum filtered; NPT, constant pressure-constant temperature ensemble; NVT,

constant volume-constant temperature ensemble; PME, particle mesh Ewald.

References

- [1] W.A. Cantara, P.F. Crain, J. Rozenski, J.A. McCloskey, K.A. Harris, X. Zhang, et al., The RNA modification database, RNAMDB: 2011 update, Nucleic Acids Res. 39 (2010) D195—D201, https://doi.org/10.1093/nar/gkq1028.
- [2] E.M. Gustilo, F.A. Vendeix, P.F. Agris, tRNA's modifications bring order to gene expression, Curr. Opin. Microbiol. 11 (2008) 134–140, https://doi.org/10.1016/j.mib.2008.02.003.
- [3] J.E. Jackman, J.D. Alfonzo, Transfer RNA modifications: nature's combinatorial chemistry playground, WIREs RNA 4 (2012) 35–48, https://doi.org/10.1002/wrna.1144.
- [4] F. Jühling, M. Mörl, R.K. Hartmann, M. Sprinzl, P.F. Stadler, J. Pütz, tRNAdb, 2009: compilation of tRNA sequences and tRNA genes, Nucleic Acids Res. 37 (2009) D159–D162, https://doi.org/10.1093/nar/gkn772.
- [5] H. Lusic, E.M. Gustilo, F.A.P. Vendeix, R. Kaiser, M.O. Delaney, W.D. Graham, et al., Synthesis and investigation of the 5-formylcytidine modified, anticodon stem and loop of the human mitochondrial tRNA^{Met}, Nucleic Acids Res. 36 (2008) 6548–6557, https://doi.org/10.1093/nar/gkn703.
- [6] C. Yarian, M. Marszalek, E. Sochacka, A. Malkiewicz, R. Guenther, A. Miskiewicz, et al., Modified nucleoside dependent Watson-Crick and wobble codon binding by tRNA Lysumus species †, Biochemistry 39 (2000) 13390–13395, https://doi.org/10.1021/bi001302g.
- [7] D.R. Davis, P.C. Durant, Nucleoside modifications affect the structure and stability of the anticodon of tRNA^{Lys3}, Nucleosides Nucleotides 18 (1999) 1579–1581.
- [8] J. Cabello-Villegas, M.E. Winkler, E.P. Nikonowicz, Solution conformations of unmodified and A₃₇N⁶-dimethylallyl modified anticodon stem-loops of Escherichia coli tRNA^{Phe}, J. Mol. Biol. 319 (2002) 1015–1034, https://doi.org/ 10.1016/S0022-2836(02)00382-0.
- [9] J. Cabello-Villegas, Solution structure of 32-modified anticodon stem-loop of Escherichia coli tRNA^{Phe}, Nucleic Acids Res. 33 (2005) 6961–6971, https://doi.org/10.1093/nar/gki1004.
- [10] A.P. Denmon, J. Wang, E.P. Nikonowicz, Conformation effects of base modification on the anticodon stem—loop of Bacillus subtilis tRNA^{Tyr}, J. Mol. Biol. 412 (2011) 285—303, https://doi.org/10.1016/j.jmb.2011.07.010.
- [11] C. Yarian, H. Townsend, W. Czestkowski, E. Sochacka, A.J. Malkiewicz, R. Guenther, et al., Accurate translation of the genetic code depends on tRNA modified nucleosides, J. Biol. Chem. 277 (2002) 16391–16395, https://doi.org/ 10.1074/jbc.M200253200.
- [12] S. Kurata, A. Weixlbaumer, T. Ohtsuki, T. Shimazaki, T. Wada, Y. Kirino, et al., Modified uridines with C5methylene substituents at the first position of the tRNA anticodon stabilize U·G wobble pairing during decoding, J. Biol. Chem. 283 (2008) 18801–18811, https://doi.org/ 10.1074/jbc.M800233200.
- [13] S.S. Phelps, A. Malkiewicz, P.F. Agris, S. Joseph, Modified nucleotides in tRNA^{Lys} and tRNA^{Val} are important for translocation, J. Mol. Biol. 338 (2004) 439–444, https:// doi.org/10.1016/j.jmb.2004.02.070.

- [14] W.A. Cantara, Y. Bilbille, J. Kim, R. Kaiser, G. Leszczyńska, A. Malkiewicz, et al., Modifications modulate anticodon loop dynamics and codon recognition of E. coli tRNA^{Arg1,2}, J. Mol. Biol. 416 (2012) 579–597, https://doi.org/10.1016/ j.jmb.2011.12.054.
- [15] S.S. Ashraf, E. Sochacka, R. Cain, R. Guenther, A. Malkiewicz, P.F. Agris, Single atom modification (O– >S) of tRNA confers ribosome binding, RNA 5 (1999) 188–194, https://doi.org/10.1017/s1355838299981529.
- [16] J. Li, B. Esberg, J.F. Curran, G.R. Björk, Three modified nucleosides present in the anticodon stem and loop influence the in vivo aa-tRNA selection in a tRNA-dependent manner, J. Mol. Biol. 271 (1997) 209–221, https://doi.org/ 10.1006/jmbi.1997.1176.
- [17] Y. Chiari, K. Dion, J. Colborn, A. Parmakelis, J.R. Powell, On the possible role of tRNA base modifications in the evolution of codon usage: queuosine and Drosophila, J. Mol. Evol. 70 (2010) 339—345, https://doi.org/10.1007/s00239-010-9329-z.
- [18] J. Ninio, Multiple stages in codon-anticodon recognition: double-trigger mechanisms and geometric constraints, Biochimie 88 (2006) 963—992, https://doi.org/10.1016/j.biochi.2006.06.002.
- [19] J. Urbonavicius, Q. Qian, J.M. Durand, T.G. Hagervall, G.R. Björk, Improvement of reading frame maintenance is a common function for several tRNA modifications, EMBO J. 20 (2001) 4863–4873, https://doi.org/10.1093/emboj/ 20.17.4863.
- [20] G.R. Björk, J.M. Durand, T.G. Hagervall, R. Leipuviene, H.K. Lundgren, K. Nilsson, et al., Transfer RNA modification: influence on translational frameshifting and metabolism, FEBS Lett. 452 (1999) 47–51, https://doi.org/10.1016/ s0014-5793(99)00528-1.
- [21] I. Brierley, M.R. Meredith, A.J. Bloys, T.G. Hagervall, Expression of a coronavirus ribosomal frameshift signal in Escherichia coli: influence of tRNA anticodon modification on frameshifting, J. Mol. Biol. 270 (1997) 360—373, https:// doi.org/10.1006/jmbi.1997.1134.
- [22] P.F. Agris, F.A.P. Vendeix, W.D. Graham, tRNA's wobble decoding of the genome: 40 Years of modification, J. Mol. Biol. 366 (2007) 1–13, https://doi.org/10.1016/ j.jmb.2006.11.046.
- [23] F.A.P. Vendeix, A. Dziergowska, E.M. Gustilo, W.D. Graham, B. Sproat, A. Malkiewicz, et al., Anticodon domain modifications contribute order to tRNA for ribosome-mediated codon binding, Biochemistry 47 (2008) 6117–6129, https://doi.org/10.1021/bi702356j.
- [24] J.W. Stuart, K.M. Koshlap, R. Guenther, P.F. Agris, Naturally-occurring modification restricts the anticodon domain conformational space of tRNA^{Phe}, J. Mol. Biol. 334 (2003) 901–918, https://doi.org/10.1016/j.jmb.2003.09.058.
- [25] M. Sundaram, P.C. Durant, D.R. Davis, Hypermodified nucleosides in the anticodon of tRNA^{Lys} stabilize a canonical U-turn structure, Biochemistry 39 (2000) 12575—12584, https://doi.org/10.1021/bi0014655.
- [26] K. Chakraburtty, Primary structure of tRNA^{Arg} of E. coli B, Nucleic Acids Res. 2 (1975) 1787–1792, https://doi.org/ 10.1093/nar/2.10.1787.
- [27] K. Murao, T. Tanabe, F. Ishii, M. Namiki, S. Nishimura, Primary sequence of arginine transfer RNA from Escherichia coli, Biochem. Biophys. Res. Commun. 47 (1972) 1332–1337, https://doi.org/10.1016/0006-291x(72)90218-5.
- [28] M. Sissler, R. Giegé, C. Florentz, Arginine aminoacylation identity is context-dependent and ensured by alternate

- recognition sets in the anticodon loop of accepting tRNA transcripts, EMBO J. 15 (1996) 5069-5076.
- [29] K. Tamura, H. Himeno, H. Asahara, T. Hasegawa, M. Shimizu, In vitro study of E.coli tRNA^{Arg} and tRNA^{Lys} identity elements, Nucleic Acids Res. 20 (1992) 2335–2339, https://doi.org/10.1093/nar/20.9.2335.
- [30] R.K. Kumar, D.R. Davis, Synthesis and studies on the effect of 2-thiouridine and 4-thiouridine on sugar conformation and RNA duplex stability, Nucleic Acids Res. 25 (1997) 1272–1280, https://doi.org/10.1093/nar/25.6.1272.
- [31] P. Romby, P. Carbon, E. Westhof, C. Ehresmann, J.P. Ebel, B. Ehresmann, et al., Importance of conserved residues for the conformation of the T-loop in tRNAs, J. Biomol. Struct. Dyn. 5 (1987) 669–687, https://doi.org/10.1080/ 07391102.1987.10506419.
- [32] J.A. McCloskey, D.E. Graham, S. Zhou, P.F. Crain, M. Ibba, J. Konisky, et al., Post-transcriptional modification in archaeal tRNAs: identities and phylogenetic relations of nucleotides from mesophilic and hyperthermophilic Methanococcales, Nucleic Acids Res. 29 (2001) 4699–4706, https://doi.org/10.1093/nar/29.22.4699.
- [33] P. Auffinger, E. Westhof, Location and Distribution of Modified Nucleotides in tRNA, Modification and Editing of RNA, 1998.
- [34] P. Boccaletto, M.A. Machnicka, E. Purta, P. Piatkowski, B. Baginski, T.K. Wirecki, et al., MODOMICS: a database of RNA modification pathways. 2017 update, Nucleic Acids Res. 46 (2018) D303–D307, https://doi.org/10.1093/nar/gkx1030.
- [35] M. Sprinzl, K.S. Vassilenko, Compilation of tRNA sequences and sequences of tRNA genes, Nucleic Acids Res. 33 (2005) D139–D140, https://doi.org/10.1093/nar/gki012.
- [36] P. Auffinger, E. Westhof, Singly and bifurcated hydrogenbonded base-pairs in tRNA anticodon hairpins and ribozymes, J. Mol. Biol. 292 (1999) 467–483, https://doi.org/ 10.1006/jmbi.1999.3080.
- [37] F.H. Crick, Codon—anticodon pairing: the wobble hypothesis, J. Mol. Biol. 19 (1966) 548–555, https://doi.org/10.1016/s0022-2836(66)80022-0.
- [38] J.F. Curran, Decoding with the A: I wobble pair is inefficient, Nucleic Acids Res. 23 (1995) 683–688, https://doi.org/ 10.1093/nar/23.4.683.
- [39] D.P. Letzring, K.M. Dean, E.J. Grayhack, Control of translation efficiency in yeast by codon-anticodon interactions, RNA 16 (2010) 2516–2528, https://doi.org/10.1261/ rna.2411710.
- [40] D.P. Letzring, A.S. Wolf, C.E. Brule, E.J. Grayhack, Translation of CGA codon repeats in yeast involves quality control components and ribosomal protein L1, RNA 19 (2013) 1208—1217, https://doi.org/10.1261/rna.039446.113.
- [41] P.C. Durant, A.C. Bajji, M. Sundaram, R.K. Kumar, D.R. Davis, Structural effects of hypermodified nucleosides in the Escherichia coli and human tRNA^{Lys} anticodon loop: the effect of nucleosides s²U, mcm⁵U, mcm⁵s²U, mnm⁵s²U, t⁶A, and ms²t⁶A, Biochemistry 44 (2005) 8078–8089, https://doi.org/10.1021/bi050343f.
- [42] S.M. Testa, M.D. Disney, D.H. Turner, R. Kierzek, Thermodynamics of RNA-RNA duplexes with 2- or 4-thiouridines: implications for antisense design and targeting a group I intron, Biochemistry 38 (1999) 16655—16662, https://doi.org/ 10.1021/bi991187d.
- [43] W. Saenger, Principles of nucleic acid structure, Springer Science & Business Media, 2013.
- [44] Y. Bilbille, F.A.P. Vendeix, R. Guenther, A. Malkiewicz, X. Ariza, J. Vilarrasa, et al., The structure of the human

- tRNA^{Lys3} anticodon bound to the HIV genome is stabilized by modified nucleosides and adjacent mismatch base pairs,, Nucleic Acids Res. 37 (2009) 3342–3353, https://doi.org/10.1093/nar/gkp187.
- [45] P.F. Agris, D. Söll, T. Seno, Biological function of 2-thiouridine in Escherichia coli glutamic acid transfer ribonucleic acid, Biochemistry 12 (1973) 4331–4337, https://doi.org/10.1021/bi00746a005.
- [46] H. Sierzputowska-Gracz, E. Sochacka, A. Malkiewicz, K. Kuo, C.W. Gehrke, P.F. Agris, Chemistry and structure of modified uridines in the anticodon, wobble position of transfer RNA are determined by thiolation, J. Am. Chem. Soc. 109 (1987) 7171–7177, https://doi.org/10.1021/ ja00257a044.
- [47] U. Baumann, W. Fischer, M. Sprinzl, Analysis of modification-dependent structural alterations in the anticodon loop of Escherichia coli tRNA^{Arg} and their effects on the translation of MS2 RNA, Eur. J. Biochem. 152 (1985) 645–649, https://doi.org/10.1111/j.1432-1033.1985.tb09243.x.
- [48] H. Shi, P.B. Moore, The crystal structure of yeast phenylalanine tRNA at 1.93 A resolution: a classic structure revisited, RNA 6 (2000) 1091–1105, https://doi.org/ 10.1017/s1355838200000364.
- [49] H. Grosjean, E. Westhof, An integrated, structure- and energy-based view of the genetic code, Nucleic Acids Res. 44 (2016) 8020–8040, https://doi.org/10.1093/nar/gkw608.
- [50] P. Auffinger, E. Westhof, An extended structural signature for the tRNA anticodon loop, RNA 7 (2001) 334–341, https:// doi.org/10.1017/s1355838201002382.
- [51] M. Olejniczak, O.C. Uhlenbeck, tRNA residues that have coevolved with their anticodon to ensure uniform and accurate codon recognition, Biochimie 88 (2006) 943–950, https://doi.org/10.1016/j.biochi.2006.06.005.
- [52] Stephen A. Scaringe, Francine E. Wincott, M.H. Caruthers, Novel RNA Synthesis Method Using 5'-O-Silyl-2'-O-Orthoester Protecting Groups, American Chemical Society, 1998, https://doi.org/10.1021/ja980730v.
- [53] S.A. Hartsel, D.E. Kitchen, S.A. Scaringe, W.S. Marshall, RNA oligonucleotide synthesis via 5"-silyl-2-"orthoester chemistry, Methods Mol. Biol. 288 (2005) 33—50.
- [54] J.M. Ogle, D.E. Brodersen, W.M. Clemons, M.J. Tarry, A.P. Carter, V. Ramakrishnan, Recognition of cognate transfer RNA by the 30S ribosomal subunit, Science 292 (2001) 897–902, https://doi.org/10.1126/science.1060612.
- [55] J.M. Ogle, F.V. Murphy, M.J. Tarry, V. Ramakrishnan, Selection of tRNA by the ribosome requires a transition from an open to a closed form, Cell 111 (2002) 721–732, https://doi.org/10.1016/s0092-8674(02)01086-3.
- [56] S.S. Ashraf, R.H. Guenther, G. Ansari, A. Malkiewicz, E. Sochacka, P.F. Agris, Role of modified nucleosides of yeast tRNA^{Phe} in ribosomal binding, Cell Biochem, Biophys 33 (2000) 241–252, https://doi.org/10.1385/CBB:47:1:159.
- [57] F.V. Murphy, V. Ramakrishnan, Structure of a purine-purine wobble base pair in the decoding center of the ribosome, Nat. Struct. Mol. Biol. 11 (2004) 1251–1252, https://doi.org/ 10.1038/nsmb866.
- [58] A. Weixlbaumer, F.V. Murphy, A. Dziergowska, A. Malkiewicz, F.A.P. Vendeix, P.F. Agris, et al., Mechanism for expanding the decoding capacity of transfer RNAs by modification of uridines, Nat. Struct. Mol. Biol. 14 (2007) 498–502, https://doi.org/10.1038/nsmb1242.
- [59] F.A.P. Vendeix, F.V. Murphy IV, W.A. Cantara, G. Leszczyńska, E.M. Gustilo, B. Sproat, et al., Human tRNALys3UUU is pre-structured by natural modifications for

- cognate and wobble codon binding through keto—enol tautomerism, J. Mol. Biol. 416 (2012) 467—485, https://doi.org/10.1016/j.jmb.2011.12.048.
- [60] A. Klug, J.D. Robertus, J.E. Ladner, R.S. Brown, J.T. Finch, Conservation of the molecular structure of yeast phenylalanine transfer RNA in two crystal forms, Proc. Natl. Acad. Sci. U.S.A. 71 (1974) 3711–3715, https://doi.org/10.1073/ pnas.71.9.3711.
- [61] G.J. Quigley, A. Rich, Structural domains of transfer RNA molecules, Science 194 (1976) 796–806, https://doi.org/ 10.1126/science.790568.
- [62] F.M. Jucker, A. Pardi, GNRA tetraloops make a U-turn, RNA 1 (1995) 219–222.
- [63] F.L. Suddath, G.J. Quigley, A. McPherson, D. Sneden, J.J. Kim, S.H. Kim, et al., Three-dimensional structure of yeast phenylalanine transfer RNA at 3. 0Å resolution, Nature 248 (1974) 20–24, https://doi.org/10.1038/248020a0.
- [64] E.M. Phizicky, A.K. Hopper, tRNA biology charges to the front, Genes Dev. 24 (2010) 1832–1860, https://doi.org/ 10.1101/gad.1956510.
- [65] J. Jaroensuk, S. Atichartpongkul, C. Yok Hian, Y.H. Wong, L. Chong Wai, M. Megan E, et al., Methylation at position 32 of tRNA catalyzed by TrmJ alters oxidative stress response in Pseudomonas aeruginosa, Nucleic Acids Res. 44 (2016) 10834–10848, https://doi.org/10.1093/nar/gkw870.
- [66] M. Sokołowski, R. Klassen, A. Bruch, R. Schaffrath, S. Glatt, Cooperativity between different tRNA modifications and their modification pathways, Biochim. Biophys. Acta - Gene Regul. Mech. 1861 (2018) 409–418, https://doi.org/ 10.1016/j.bbagrm.2017.12.003.
- [67] L. Pintard, F. Lecointe, J.M. Bujnicki, C. Bonnerot, H. Grosjean, B. Lapeyre, Trm7p catalyses the formation of two 2'-O-methylriboses in yeast tRNA anticodon loop, EMBO J. 21 (2002) 1811–1820, https://doi.org/10.1093/ emboj/21.7.1811.
- [68] Y. Yamada, M. Saneyoshi, S. Nishimura, H. Ishikura, Isolation and characterization of 2-thiocytidine from a serine transfer ribonucleic acid of Escherichia coli, FEBS Lett. 7 (1970) 207–210, https://doi.org/10.1016/0014-5793(70) 80161-2.
- [69] G. Jäger, R. Leipuviene, M.G. Pollard, Q. Qian, G.R. Björk, The conserved cys-X₁-X₂-cys motif present in the TtcA protein is required for the thiolation of cytidine in position 32 of tRNA from Salmonella enterica serovar typhimurium, J. Bacteriol. 186 (2004) 750–757, https://doi.org/10.1128/ JB.186.3.750-757.2004.
- [70] W. Deng, I.R. Babu, D. Su, S. Yin, T.J. Begley, P.C. Dedon, Trm9-catalyzed tRNA modifications regulate global protein expression by codon-biased translation, PLoS Genet. 11 (2015), e1005706, https://doi.org/10.1371/journal.pgen.1005706.
- [71] C. Gu, T.J. Begley, P.C. Dedon, tRNA modifications regulate translation during cellular stress, FEBS Lett. 588 (2014) 4287–4296, https://doi.org/10.1016/j.febslet.2014.09.038.
- [72] P.C. Dedon, T.J. Begley, A system of RNA modifications and biased codon use controls cellular stress response at the level of translation, Chem. Res. Toxicol. 27 (2014) 330—337, https://doi.org/10.1021/tx400438d.
- [73] L. Endres, P.C. Dedon, T.J. Begley, Codon-biased translation can be regulated by wobble-base tRNA modification systems during cellular stress responses, RNA Biol. 12 (2015) 603-614, https://doi.org/10.1080/15476286.2015.1031947.

- [74] J.F. Kane, Effects of rare codon clusters on high-level expression of heterologous proteins in Escherichia coli, Curr. Opin. Biotechnol. 6 (1995) 494–500.
- [75] A.S. Wolf, E.J. Grayhack, Asc1, homolog of human RACK1, prevents frameshifting in yeast by ribosomes stalled at CGA codon repeats, RNA 21 (2015) 935–945, https://doi.org/ 10.1261/rna.049080.114.
- [76] T.E.F. Quax, N.J. Claassens, D. Söll, J. van der Oost, Codon Bbias as a means to fine-tune gene expression, Mol. Cell 59 (2015) 149–161, https://doi.org/10.1016/j.mol-cel.2015.05.035.
- [77] G. Pixa, G. Dirheimer, G. Keith, Sequence of tRNAl^{IQ} from brewer's yeast, Biochem. Biophys. Res. Commun. 119 (1984) 905–912, https://doi.org/10.1016/0006-291x(84) 90859-3.
- [78] T.R. Sosnick, Characterization of tertiary folding of RNA by circular dichroism and urea, Curr. Protoc. Nucleic Acid Chem. 4 (2001), https://doi.org/10.1002/ 0471142700.nc1105s04, 11.5.1—11.5.10.
- [79] I. Wong, T.M. Lohman, A double-filter method for nitrocellulose-filter binding: application to protein-nucleic acid interactions, Proc. Natl. Acad. Sci. U.S.A. 90 (1993) 5428–5432, https://doi.org/10.1073/pnas.90.12.5428.
- [80] R.P. Fahlman, T. Dale, O.C. Uhlenbeck, Uniform binding of aminoacylated transfer RNAs to the ribosomal A and P sites, Mol. Cell 16 (2004) 799–805, https://doi.org/10.1016/j.molcel.2004.10.030.
- [81] P. Leder, H. Bursztyn, Initiation of protein synthesis: the role of formyl-accepting methionyl-tRNA, Cold Spring Harbor Symp. Quant. Biol. 31 (1966) 297–301, https://doi.org/ 10.1101/sqb.1966.031.01.039.
- [82] B. Maurizio, X. Liquin, M. Alexander, 23S rRNA positions essential for tRNA binding in ribosomal functional sites, Proc. Natl. Acad. Sci. U.S.A. 95 (1998) 3525–3530.
- [83] R. Rakauskaite, J.D. Dinman, rRNA mutants in the yeast peptidyltransferase center reveal allosteric information networks and mechanisms of drug resistance, Nucleic Acids Res. 36 (2008) 1497–1507, https://doi.org/10.1093/nar/ gkm1179.
- [84] D. Das, D. Samanta, A. Bhattacharya, A. Basu, A. Das, J. Ghosh, et al., A possible role of the full-length nascent protein in post-translational ribosome recycling,, PLoS One 12 (2017), e0170333, https://doi.org/10.1371/journal.pone.0170333.
- [85] W.M. Clemons, D.E. Brodersen, J.P. McCutcheon, J.L. May, A.P. Carter, R.J. Morgan-Warren, et al., Crystal structure of the 30 S ribosomal subunit from Thermus thermophilus: purification, crystallization and structure determination, J. Mol. Biol. 310 (2001) 827–843, https://doi.org/10.1006/ jmbi.2001.4778.
- [86] W. Kabsch, IUCr, Automatic processing of rotation diffraction data from crystals of initially unknown symmetry and cell

- constants, J. Appl. Crystallogr. 26 (1993) 795–800, https://doi.org/10.1107/S0021889893005588.
- [87] P.D. Adams, P.V. Afonine, G. Bunkóczi, V.B. Chen, I.W. Davis, N. Echols, et al., PHENIX: a comprehensive Python-based system for macromolecular structure solution, Acta Crystallogr, D Biol. Crystallogr. 66 (2010) 213–221, https://doi.org/10.1107/S0907444909052925.
- [88] P. Emsley, K. Cowtan, Coot: model-building tools for molecular graphics, Acta Crystallogr, D Biol. Crystallogr. 60 (2004) 2126–2132, https://doi.org/10.1107/ S0907444904019158.
- [89] W.L. DeLano. The PyMol Molecular Graphics System, Delano Scientific, San Carlos, CA, USA, 2002.
- [90] N.W. Moriarty, R.W. Grosse-Kunstleve, P.D. Adams, Electronic Ligand Builder and Optimization Workbench (eL-BOW): a tool for ligand coordinate and restraint generation, Acta Crystallogr. D Biol. Crystallogr. 65 (2009) 1074–1080, https://doi.org/10.1107/S0907444909029436.
- [91] W.D. Cornell, P. Cieplak, C.I. Bayly, I.R. Gould, K.M. Merz, D.M. Ferguson, et al., A second generation force field for the simulation of proteins, nucleic acids, and organic molecules, J. Am. Chem. Soc. 117 (1995) 5179–5197, https://doi.org/ 10.1021/ja00124a002.
- [92] A.A. Chen, A.E. García, High-resolution reversible folding of hyperstable RNA tetraloops using molecular dynamics simulations, Proc. Natl. Acad. Sci. U. S. A. 110 (2013) 16820–16825, https://doi.org/10.1073/pnas.1309392110.
- [93] MOE (The Molecular Operating Environment) Version 2013.08, (August 2013).
- [94] B. Hess, C. Kutzner, D. van der Spoel, E. Lindahl, GROMACS 4: Algorithms for highly efficient, load-balanced, and scalable molecular simulation, J. Chem. Theory Comput. 4 (2008) 435–447, https://doi.org/10.1021/ct700301q.
- [95] G. Bussi, D. Donadio, M. Parrinello, Canonical sampling through velocity rescaling, J. Chem. Phys. 126 (2007), https://doi.org/10.1063/1.2408420, 014101.
- [96] H.J.C. Berendsen, J.P.M. Postma, W.F. van Gunsteren, A. DiNola, J.R. Haak, Molecular dynamics with coupling to an external bath, J. Chem. Phys. 81 (1998) 3684—3690, https://doi.org/10.1063/1.448118.
- [97] M. Parrinello, A. Rahman, Polymorphic transitions in single crystals: A new molecular dynamics method, J. Appl. Phys. 52 (1998) 7182–7190, https://doi.org/10.1063/1.328693.
- [98] T. Darden, D. York, L. Pedersen, Particle mesh Ewald: An N·log(N) method for Ewald sums in large systems, J. Chem. Phys. 98 (1998) 10089–10092, https://doi.org/10.1063/ 1.464397.
- [99] B. Hess, H. Bekker, H.J.C. Berendsen, J.G.E.M. Fraaije, LINCS: A linear constraint solver for molecular simulations, J. Comput. Chem. 18 (1997) 1463–1472, https://doi.org/ 10.1002/(SICI)1096-987X(199709)18:12<1463::AID-JCC4>3.3.CO;2-L.